13777

# TARDEC

*---TECHNICAL REPORT---*

THE NATION'S LABORATORY FOR ADVANCED AUTOMOTIVE TECHNOLOGY

No. 13777


WINNER OF THE 1995 PRESIDENTIAL AWARD FOR QUALITY

# Modeling and Simulation of a Differential Torque Steered Wheeled Vehicle



By William R. Meldrum
Francis B. Hoogterp
Alexander R. Kovnat

U.S. Army Tank-Automotive Research,
Development, and Engineering Center
Detroit Arsenal
Warren, Michigan 48397-5000

# REPORT DOCUMENTATION PAGE

*Form Approved*
*OMB No. 074-0188*



| 1. AGENCY USE ONLY (Leave blank) | 2. REPORT DATE | 3. REPORT TYPE AND DATES COVERED |
|---|---|---|
| | 5 October, 1999 | TARDEC Technical Report |

**4. TITLE AND SUBTITLE**
Modeling and Simulation of a Differential Torque Steered Wheeled Vehicle

**5. FUNDING NUMBERS**

**6. AUTHOR(S)**
William R. Meldrum
Francis B. Hoogterp
Alexander R. Kovnat

**7. PERFORMING ORGANIZATION NAME(S) AND ADDRESS(ES)**
U.S. Army TARDEC
AMSTA-TR-R/MS159
Warren MI, 48397-5000

**8. PERFORMING ORGANIZATION REPORT NUMBER**
13777

**9. SPONSORING / MONITORING AGENCY NAME(S) AND ADDRESS(ES)**

**10. SPONSORING / MONITORING AGENCY REPORT NUMBER**

**11. SUPPLEMENTARY NOTES**

**12a. DISTRIBUTION / AVAILABILITY STATEMENT**
Distribution Statement A:
Approved For Public Release: Distribution is Unlimited

**12b. DISTRIBUTION CODE**
A

**13. ABSTRACT** ***(Maximum 200 Words)***

This paper discusses the evolution of skid steer systems, and takes a new look at the advantages and implications of designing future ground combat vehicles with all non-steerable wheels. The traditional "skid steer" designation of such vehicles is dropped in favor of the more descriptive phrase "differential torque steer" vehicle. The possible advantages of such systems for combat vehicle application are presented along with a synopsis of various past modeling, simulation, and vehicle hardware efforts to evaluate skid steer systems. A comprehensive vehicle modeling effort for a differential torque steer system is then presented. Two independent implementations of the model are presented along with model verification and validation results. Finally the model is used to evaluate potential turning performance for a 4x4 vehicle with differential torque steer.

| 14. SUBJECT TERMS | 15. NUMBER OF PAGES |
|---|---|
| | 40 |
| | 16. PRICE CODE |

| 17. SECURITY CLASSIFICATION OF REPORT | 18. SECURITY CLASSIFICATION OF THIS PAGE | 19. SECURITY CLASSIFICATION OF ABSTRACT | 20. LIMITATION OF ABSTRACT |
|---|---|---|---|
| | | | |

Technical Report 13777
July 1999

# Modeling and Simulation of a Differential Torque Steered Wheeled Vehicle

by William R. Meldrum
Francis B. Hoogterp
Alexander R. Kovnat

U.S. Army Tank-Automotive Research, Development and Engineering Center
ATTN: AMSTA-TR-R/MS159
Warren, MI 48397-5000

TABLE OF CONTENTS

List of Figures

## ABSTRACT

This report presents two separate three dimensional vehicle models that have been developed to study the performance capabilities and potential of wheeled vehicles with non-steerable wheels (traditionally called skid steered vehicles). The possible military advantages of non-steerable wheels on a vehicle is discussed, along with the results of a comprehensive literature search on skid steer technology for wheeled vehicles. The two vehicle models were developed in MATLAB and DADS respectively to represent a pair of 4x4 Army vehicle concepts, the HMMWV and an LAV derivative. The various model elements, vehicle input data, model output capability, and tire-ground interface representation is all discussed. A variety of verification and cross-comparable simulation results are also presented along with a brief discussion of future validation efforts and applications of the model.

## INTRODUCTION

The following sections discuss the meaning and historical significance of skid steer systems, and make a case for vehicles with all non-steerable wheels to abandon the "skid steer" designation in favor of the more descriptive phrase "differential torque steer". The possible advantages of such systems for combat vehicle application are discussed along with various modeling, simulation, and vehicle hardware efforts to evaluate skid steer systems. Later sections document a more comprehensive vehicle modeling and simulation effort. Two independent implementations of the model are presented, along with model verification and validation results.

### Skid—differential torque steer

Track laying vehicles have, of necessity, always employed what has traditionally been labeled skid steering. Since a tracked vehicle has no provision for turning the track about the vehicle yaw axis, (except possibly in an articulated, multi-track design), it must rely on changing the relative torque (or speed) of the two tracks in order to generate a vehicle yaw moment to turn the vehicle. In the simplest systems, the inside track is braked to provide such a turning moment. This causes the vehicle to skid about the braked track, thus leading to the term "skid steer". Modern tracked vehicles employ transmissions that permit power absorbed by the inner track to be transferred to the outer track, greatly reducing the power required in turning maneuvers [1]. If the two tracks can be driven in opposite directions simultaneously, the vehicle can perform what is called a pivot steer maneuver in which it simply spins about a stationary vertical axis. Each of these configurations has retained the designation of "skid steer" systems.

Many low speed wheeled vehicles have also employed skid steer systems. Agricultural tractors, though they have steerable front wheels, are often equipped with individual brakes for the two sides of the vehicle to provide a combined steering effect. This permits a much smaller radius of turn than can be accomplished by only steering the front wheels. Many load handling vehicles, such as highlows and small front end loaders

are also designed with non-steerable wheels and rely on skid steering to turn the vehicle. Limited efforts have also been made to adapt skid steering to military wheeled vehicles. The UK built a 6x6 skid steered wheeled test bed in the 1980s. France actually fielded a 6x6 armored vehicle (the AMX 10 RC) with skid steering. More recently France has developed the MODIX, an 8x8 steering research vehicle, which will be used to evaluate alternative steering approaches for wheeled vehicles.

The increasing prospect of electric drive vehicles and the development of individual wheel traction motors, opens up the possibility of designing higher performance skid steer systems. The use of separate traction motors at each wheel implies that torque to each wheel can be independently controlled. It also provides a system that is regenerative by nature. By using motor braking, the power absorbed at one wheel is available for application at an opposing wheel.

The concept of independently controlling the torque of each wheel to effect vehicle steering will permit a smooth transition from power consuming low speed turns to the more moderate efforts required for high speed on-road operation. It is conjectured that such a system can be controlled without the characteristic feeling of instability generated by operation of a skid steer system at higher speeds. Such a system might more appropriately be termed a "differential torque steer" rather than a "skid steer" system.

**Need for skid steer**

Design requirements for combat vehicles take on many different aspects. It is precisely the trade-off between different requirements that drives the selection between tracked and wheeled vehicles for a particular application. Since combat vehicles typically have a large off-road mission requirement, cross-country mobility is always critical. Speed and agility are also important, as are armor protection and useable interior volume. The vehicle must also meet certain transportability specifications, which limit the physical dimensions and weight of the system. In the past, combat vehicles have predominately been tracked, rather than wheeled vehicles. Tracked vehicles can generally be designed to achieve somewhat higher soft soil and obstacle crossing capability. This is accomplished however, at the expense of having a less fuel efficient, noisier, and significantly slower travelling vehicle than could be achieved with a comparable wheeled concept.

One additional consideration that has tended to favor a tracked rather than a wheeled vehicle design, is the broadly held conception that a tracked system takes less chassis (or hull) volume than does a comparable wheeled system. This is important since the outside vehicle dimensions are bounded by transportability requirements and running gear (i.e. track or wheel system) volume takes away from useable interior vehicle volume. The assumption of less volume for a tracked system, however, is based on a wheeled vehicle with a conventional steering system. The swept volume required by a steerable wheel is quite significant and grows with tire size. A differential torque steer system with non-steerable tires would negate this volume argument and would additionally provide the vehicle with pivot steer capability normally only achievable with tracked vehicles. The

advantages of such a wheeled vehicle design would be; higher speeds, quieter operation, and better fuel economy. Also, there would be a significantly lower operation and maintenance costs for tires rather than for tracks. However, a skid steered wheeled vehicle design would also come with the disadvantage of slightly degraded soft soil and obstacle crossing capability compared to a tracked vehicle.

It is the advantages of the wheeled vehicle that has led to a resurgence of interest in skid steering for wheeled combat vehicles. The next section discusses various efforts to model and simulate skid steer systems.

**Previous skid steer modeling**

Mangialardi and Gentile [2-4] have written several papers on the subject of skid steered vehicles. Methods of analysis used in their papers are characterized by neglecting aerodynamics, assuming a rigid vehicle frame, and stipulating that the vehicle remains parallel to the ground during cornering.

In [2] Mangialardi models a 4x4 skid steered vehicle. Differential equations are developed for the chassis fore-aft, side-to-side, and yaw motions. Three second order differential equations describe these accelerations. The equations of motion are driven by the calculated wheel speeds needed to maintain the specified maneuver. The tire-ground interface is represented in terms of maximum lateral and longitudinal coefficients of friction. The combined maximum coefficient of friction is governed, however, by an elliptical equation of the type:

$$\mu^2_{x,R} / \mu^2_{x,0} + \mu^2_{y,R} / \mu^2_{y,90} = 1 \qquad (1)$$

where $\mu_{x,R}$ and $\mu_{y,R}$ are the instantaneous longitudinal and lateral tire coefficients of friction at the side slip angle R, $\mu_{x,0}$ is the longitudinal tire coefficient of friction in the absence of side slip, while $\mu_{y,90}$ is the corresponding lateral coefficient of friction that would result if one were to push sideways on a tire (i.e. at an angle of 90 degrees relative to the tire's rolling direction).

It is assumed that when the skid-steered vehicle is turning, the lateral and longitudinal forces exceed the maximum limits imposed by tire coefficients of friction. Hence one can calculate lateral and longitudinal forces on the wheels if wheel loads are known. Vertical wheel load is calculated from static weight distribution. Inertial forces which transfer weight forward/rearward, and from one side to another (without consideration of suspension characteristics) are also included.

The model was used to simulate a 4x4 skid steered vehicle with various values of longitudinal and lateral tire coefficients of friction. Not surprisingly, lower lateral coefficients of friction increased the turning capability of the vehicle.

Later Gentile and Mangialardi described a BASIC computer code named STAB, which calculates the behavior of a two-axle skid-steer vehicle traveling a constant-radius circle

[3]. The transitional period between straight line and the circular path motion is also addressed.

This model assumes the vehicle is symmetric about its longitudinal axis and that it operates on a firm flat surface. Tire and suspension vertical compliance is not considered. The vehicle model includes three second order differential equations describing fore-aft, side-to-side, and chassis yaw motions. The tires are modeled in terms of their longitudinal and lateral coefficients of friction.

The velocities of the wheels on one side of the vehicle are assumed to be the same (much as if they were encircled by a track). Thus the theoretical radius of turn assumed by a skid-steer (or tracked) vehicle is given by:

$$R = ((v_o+v_i)/(v_o-v_i))*b/2 \qquad (2)$$

where b is the distance between tires on the right and left sides of the vehicle, and $v_o$ and $v_i$ are the velocities of the outer and inner tires respectively. This theoretical value is less than the radius calculated when side slip is taken into account.

The model is used to study transient effects for three cases: with the inner wheels braked (This is the only steering method one could use with a clutch-brake system), by simultaneously speeding up the outer wheels and slowing down inner wheels, and by only speeding up the outer wheels. Parameters are chosen such that each case has the same final equilibrium turning circle diameter. It is found that simultaneously speeding up the wheels on the outside and slowing down the wheels on the inside of the turn by a like amount, minimizes transients. During transition from steady rectilinear to uniform circular motion the vehicle noses inward or oversteers. This also occurs with tracked vehicles.

Finally Gentile and Mangialardi extend the 4x4 skid steer model described in [3] to accommodate a variable number of axles [4]. This model is used to study the effect of number of axles on power requirements, distribution of tire forces, and tire wear. Three axles were found to be optimum for skid steered vehicles, in that engine power requirement and tire wear are minimized.

Creedy also developed a wheeled vehicle skid steer model, which was implemented in BASIC [5]. The model assumes an N-wheeled vehicle, (N is an even number), where vertical wheel loads are calculated using CG forces and input torques applied to each wheel. It is once again assumed that the ground surface is flat and unyielding although not necessarily horizontal. Tire flexibility is not considered and the tire lateral and longitudinal forces are modeled independently as a coulomb friction interface. Equations are derived based on an equilibrium solution to a steady state turning maneuver. The equations consist of a complex set of partial differential equations to describe the circular motion of a skid steered vehicle on a hard surface.

The wheels on each side of the vehicle are treated as though they constituted a "track", which rotates faster than it otherwise would if on the outside of a turn, or slower than it otherwise would if on the inside of the same turn. The steering ratio S is defined as the ratio of the rotational speeds of the faster and slower side. If S = -1, we have pivot turn. Rotational speed is analogous to track velocity relative to the hull for a tracked vehicle.

This model also permits the calculation of steering performance on slopes. A model of a skid steer vehicle on a slope is presented, with an arbitrary slope angle relative to a gravitationally level plane, and with the vehicle at an arbitrary orientation relative to straight uphill. The vehicle is assumed to be turning toward the uphill vector and operating at low speed. Vehicle weight is resolved into components normal to the plane, and two more components parallel to the vehicle's longitudinal and lateral axes passing through the center of gravity. For some heading angles it is shown that skid steering is not possible when slope angle equals or exceeds a certain limit. As limits of vehicle performance are reached on steep slopes, one can expect a substantial increase in radius needed for turning, as one needs most of the available propulsive forces and power simply to fight the slope.

The simulated results for a 6x6 were compared with measurements conducted on an actual vehicle, the TV1000, a 6x6 vehicle built by the United Kingdom Military Vehicles and Engineering Establishment to investigate skid steering. The theory gives good agreement with the test results only at low radius of turns. Calculated torques at higher radii of turn attained in fourth gear, are up to 175% greater than the measured torques. The possible reason postulated for this is that the model neglects lateral flexibility of the tires. There was good agreement between theory and experiment, regarding power input to the wheels. Tests were conducted with the transmission in neutral (providing a pivot steer), and in all of the four forward gears.

An 8x8 skid steered vehicle concept; designated TV1333 was also modeled. It was assumed to weigh 10% more than the TV1000. The simulated 8x8 skid steered vehicle did not offer notable steering improvement over the 6x6 configuration.

The methods developed for this wheeled vehicle model were also applied to a hypothetical comparable tracked vehicle, designated TV6000. The TV6000 was assumed to have 12 road wheels. The simulated steering performance of the 6x6 and the 8x8 wheeled vehicles were compared with that of the 12 roadwheel tracked concept. These results indicated that the wheeled vehicles required a greater speed difference and more power input to maintain a steady turn, than did the tracked vehicle. The tracked vehicle also handled slopes better.

Schmid and Tomaske were motivated to look at skid steering by recent developments in electric drive motors which would allow each wheel to be independently controlled [6]. The focus of this effort was a 36-ton, 8x8 vehicle with skid steer. Vehicles with a steerable front axle, and steerable front and rear axles were also included as part of the study.

The vehicle model is derived based on a steady state turning maneuver for a symmetrically arranged (longitudinally speaking) set of axles. The side slip angles for the front and rear wheels on the same side of the vehicle are assumed to be equal in magnitude and opposite in sign to each other, and are calculated based on a steady-state turn of a given radius. The lateral tire forces are thought of as causing resistance to turning, which is overcome by the differential longitudinal (or tractive) forces between the two sides of the vehicle. Only horizontal plane motion is considered and the lateral and longitudinal tire force induced yaw moments are balanced to provide the indicated yaw acceleration.

Based on the required tire side slip angles, it is shown that for large radius turns (35 meters or more), tires absorb cornering deflection by elastic deflection. For progressively smaller radii, frictional deflection comes increasingly into play. For radii 15 meters or less, the tires slide sideways and the tire lateral force becomes purely frictional. The tire model allows for this varying effect as the vehicle turning radius varies. Unlike other authors who assume that all wheels on one side rotate at the same speeds, this model assumes instead that wheel torques on a given side are equal.

The maximum tire force achievable in the horizontal plane is governed by the force circle (note the assumption of a uniform coefficient of friction $\mu$ for all directions of tire sliding changes the more general ellipse into a circle) equation as follows:

$$F^2_{max} = \mu^2 F_z^2 = f_x^2 + f_y^2 \qquad (3)$$

where $f_x$ is the tire longitudinal force, $f_y$ is the tire lateral force, $\mu$ is the tire coefficient of friction, and $F_z$ is the vertical load acting upon the tire. This force circle represents the interaction between the longitudinal and lateral tire forces caused by the simultaneous tire slip in the two directions.

The most comprehensive of the skid steer modeling efforts reviewed was due to Renou and Chavant [7]. Actually two complimentary models were reported. A steady state, skid steer model for a constant radius turn was developed on a PC and a more complete dynamic model was written in ADAMS, a multibody software package. The dynamic model was developed by SERA, a French research society specializing in vehicle dynamics. Their skid steering and tire models were integrated into the ADAMS dynamic model.

These models were developed to simulate the French AMX10RC. The AMX10RC is a production armored vehicle of the French Army. It is a 6x6 wheel vehicle, which relies solely on skid steering for its directional control. Simulation results were compared with steering tests performed with the actual vehicle.

The same tire model was used for both the steady state and dynamic models. It was based on actual tire test data to obtain lateral and longitudinal forces as functions of side slip and speed ratio (or longitudinal slip). This model also used the friction ellipse to represent the interdependency of lateral and longitudinal tire forces.

The steady state theory is based on the force equilibrium equations for lateral and yaw motions in a constant radius turning maneuver. The yaw moment due to differential longitudinal forces on the right and left sides is balanced by the vector sum of the resisting moments due to lateral forces acting on all wheels. Also, the sum of lateral forces is set equal to the cornering acceleration $mv^2/r$.

Renou and Chavant also describe steering tests with an actual AMX10RC, conducted on a concrete surface. For each of four gearbox ratios, a pivot turn and a finite radius turn were carried out and various parameters measured. Results of measurements carried out in second gear were compared with the results of the steady state computer model. Agreement was quite good, considering uncertainties in theory and measurement. Test results for the two higher gear ratios were not compared since the vehicle was prone to oversteer in these gears, so steady state results were not obtained.

The dynamic model is more briefly described and only a single set of transient response time signals from this model is compared with the similar vehicle test signals. One important need identified from the development and use of these models, is a better model and data for tire behavior at high slip angles and large slip ratios (wheel speed to actual speed).

In a subsequent effort, Renou teamed with Durand and Favero to document a French steering research vehicle [8]. They discuss an 8x8 vehicle that can be steered conventionally or by skid steering. This vehicle is called MODIX, and was developed by the French armed forces procurement agency DGA. The prime mover for MODIX is a Mercedes OM444LA engine driving hydraulic pumps for propulsion and steering functions.

Each wheel has independent wishbones, a steering rod (for conventional steering), and a hydraulic motor driving the hub via a two-speed gearbox. Suspension is by spring and shock absorber with bump and rebound stops. Each wheel also is provided with a hydraulic disc brake. The steering rod is actuator controlled by a steer by wire system. An on-board computer permits operator selection of the desired steering configuration. The computer, a Motorola 68040, also controls the load on each wheel via a hydraulic jack and the speed of each wheel through its individual hydraulic hub motor.

A complete model of MODIX has been developed using PROSPER. It was necessary to develop a model for MODIX's hydrostatic transmission system, to accurately simulate its performance characteristics. The computer model together with the highly instrumented MODIX will be used to experiment and simulate various options for future wheeled vehicle designs. As of this writing, the results of any such investigations were not readily available for analysis.

## VEHICLE MODELS

The lack of reliable test data for skid-steer wheeled vehicle systems precipitated the development of two distinctly different approaches to modeling such a vehicle. These two approaches were adopted to help verify performance results until appropriate vehicle test data could be obtained to more formally validate the models. The first model was developed using the commercially available DADS multibody dynamics modeling software [9]. The second approach was the development of a vehicle model in MATLAB [10]. The models resulting from these approaches are discussed in the following sections.

### DADS skid steer vehicle model

The DADS model was developed to represent a vehicle of the same class as the Marine Corp LAV vehicle. The LAV is an 8x8 with steering on the front two axles. The LAV is equipped with a double A-arm suspension on the two front axles, and a torsion bar suspension on the rear axles. The concept vehicle evaluated here was designed to provide as much internal hull volume as possible. With this in mind, the DADS model of the concept was given a torsion bar suspension at all wheel stations. The replacement of the double A arm on the front two wheels with torsion bars saves internal volume, but at the cost of not allowing the wheels to be steerable.

In order for the DADS model to resemble the MATLAB model, the concept vehicle initially had the middle wheel stations removed. This reduces the concept to a 4x4 and makes it more comparable to the 4x4 vehicle modeled in MATLAB that is discussed below. To allow the same spring and damper curves to be effective on the LAV derivative, the overall vehicle weight was reduced by 50%. With this change, the wheel stations still have the same static load. Similarly, the pitch, roll, and yaw hull inertias were also appropriately reduced.

The model consists of 9 individual rigid bodies: the chassis, four roadarms, and four wheels. The roadarms are connected to the chassis, and the wheels are connected to the roadarms with revolute joints. The torsion bars are modeled as non-linear rotational springs and the dampers are modeled as translational dampers. Use of electric hub motors at each wheel station was a primary objective. To achieve this flexibility a torque time history is applied separately to each wheel. It is assumed that the vehicle operates over a hard flat surface.

The tires were modeled using the FULL tire model. This is the most comprehensive tire model available in DADS. It calculates rotational inertia as well as the effects of the suspension and steering system on the steer and camber angles of the tire. The tire normal, longitudinal, and lateral forces are then calculated in the tire/ground interface plane.

The longitudinal tire force is calculated as a function of rotational slip as,

$$F_{long} = F_N * \mu_{long} * \text{sign}(Rslip) + Torque / R \quad (4)$$

where $F_N$ is the normal force, $\mu_{long}$ is the longitudinal friction coefficient, Rslip is the rotational slip of the wheel, Torque is the torque about the wheel, and R is the deformed radius of the tire. The longitudinal friction coefficient is represented as a piece-wise linear function of rotational slip, based upon the nominal friction coefficient $\mu$. This function is shown in Figure 1. The rotational slip ratio is defined as the percent difference in velocity between the bottom point of the tire and the wheel center.

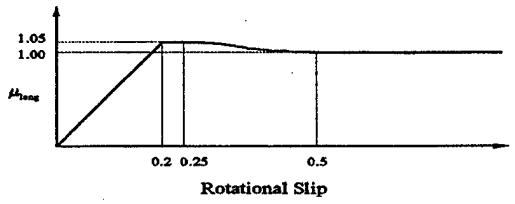


**Figure 1 Rotational slip for DADS tire model**

The lateral force, $F_{lat}$, is calculated as a function of side slip angle. Side slip is the angle formed between the tire center heading vector and the tire velocity vector. The tire characteristics are provided to DADS in terms of the coefficient of friction and the tire cornering stiffness. With this information and the side slip angle that is calculated, the program uses a cubic approximation of a carpet plot to calculate $F_{lat}$.

DADS initially calculates $F_{long}$ and $F_{lat}$ separately. However these forces are not completely independent of one another. After values for $F_{long}$ and $F_{lat}$ are obtained, DADS computes the friction ellipse limits for the vehicle and appropriately reduces the longitudinal and lateral forces if necessary.

**MATLAB skid steer vehicle model**

The theory for a skid steer, wheeled vehicle model was also derived and implemented using MATLAB [11-12]. The model was developed to permit the evaluation of any transient maneuver that might be defined and to subsequently permit the ready addition of drive torque control to effect given maneuvers. The model includes a complete 6

degree-of-freedom description of the chassis along with the vertical and rotational motions for each wheel. Each degree of freedom is described by its appropriate second order differential equation (except for the wheel rotational motion, which omits angular displacement and is therefore only first order). The vehicle is assumed to operate on a hard, flat, horizontal surface. The model accounts for suspension and tire deflections, as well as a 3 dimensional tire-ground interface model.

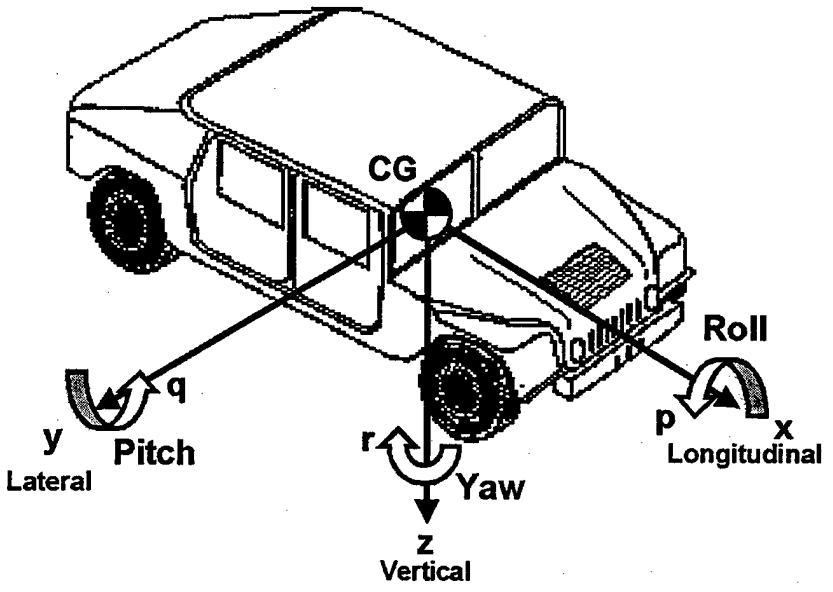


**Figure 2 SAE Vehicle Coordinate system**

The SAE standard vehicle coordinate system is assumed as depicted in Figure 2. This vehicle coordinate system is coincident with the global coordinate system at the beginning of the simulation. The model is initialized to the specified vehicle velocity in a steady state straight-ahead direction, along the global x-axis. The model input is provided in terms of a desired torque time history for each wheel. The differential equations describing the various motions are described in the paragraphs below.

The vertical motion of the chassis center of gravity (cg) is given by:

$$Z''_{cg} = g - \left( \sum_i F_{si} \right) / m_s \qquad (5)$$

where $Z_{cg}$ is the chassis cg vertical position, $F_{si}$ is the total suspension force at wheel i, $m_s$ is the chassis sprung mass, and g is the gravitational constant. The summation is over all the wheels (4 in the case of the HMMWV).

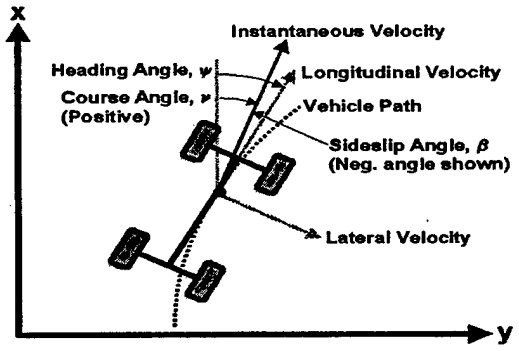


**Figure 3 Vehicle motion in global x-y coordinate system**

The linear chassis motion in the horizontal ground plane is described by two separate differential equations. The global x and y-axes initially have their origins at the vehicle chassis cg and are oriented forward along the vehicle's roll axis and to the right along the pitch axis. The vehicle's motion in the global ground plane is depicted in Figure 3. The chassis cg motion along the global x and y axes are described by the following two differential equations:

$$X''_{cg} = F_x / m_{tot} \tag{6}$$

$$Y''_{cg} = F_y / m_{tot} \tag{7}$$

where $X_{cg}$ and $Y_{cg}$ are the chassis positions in the global x and y directions respectively, $F_x$ and $F_y$ are the total ground plane forces in the global x and y directions, and $m_{tot}$ is the total mass of the vehicle (sprung plus unsprung). The global tire-ground forces, $F_x$ and $F_y$, are obtained from the summation of the appropriate components of the individual tire longitudinal and lateral forces and are given by the following equations:

$$F_x = \left(\sum_i F_{ilat}\right) \sin(\psi) + \left(\sum_i F_{ilong}\right) \cos(\psi) \quad (8)$$

$$F_y = \left(\sum_i F_{ilat}\right) \cos(\psi) + \left(\sum_i F_{ilong}\right) \sin(\psi) \quad (9)$$

where $F_{ilat}$ and $F_{ilong}$ are the lateral and longitudinal tire forces for each tire i, the summation is again over all the tires, and $\psi$ is the chassis yaw angle with respect to the global axes. The tire forces, $F_{ilat}$ and $F_{ilong}$, are the reaction forces transmitted by the road upon each tire along that tire's Y' and X' axes shown in Figure 4.

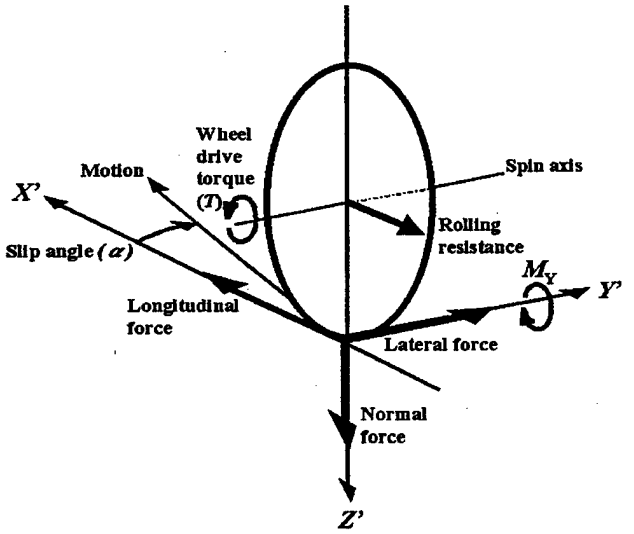


**Figure 4 Tire coordinate system and forces**

The chassis roll, pitch, and yaw angles (i.e. $\phi$, $\theta$, and $\psi$) are defined as the rotational motions about the vehicle x, y, and z axes respectively where the vehicle longitudinal and lateral axes (i.e. the x and y) stay nearly horizontal and the vehicle z-axis remains almost vertical. The differential equations defining these angular accelerations are as follows:

$$\phi'' = \sum_i \left(L_{\phi i} F_{si} - h_{cg} F_{ilat}\right) / J_\phi \quad (10)$$

$$\theta'' = \sum_i \left(L_{\theta i} F_{si} + h_{cgh} F_{ilong}\right) / J_\theta \quad (11)$$

$$'' = \sum_i \left(L_{\phi i} F_{ilong} - L_{\theta i} F_{ilat}\right) / J_\psi \quad (12)$$

where $L_{\phi i}$, $L_{\theta i}$, and $L_{\psi i}$ are the roll, pitch, and yaw moment arms from the chassis cg to each wheel respectively; $h_{cg}$ and $h_{cgh}$ are the vertical distances of the cg from the ground and from the wheel hubs; and $J_\phi$ and $J_\theta$ are the chassis sprung roll and pitch moments of inertia and $J_\psi$ is the total vehicle's yaw moment of inertia.

The final two differential equations describe the relevant wheel motions. The vertical acceleration of each wheel in the vehicle coordinate system (also in the tire coordinate system since the z-axes of the two systems always align) is given by the following:

$$Z_{ti}'' = g + \left(F_{ki} + F_{bi} - F_{ti}\right) / m_w \quad (13)$$

where $F_{ki}$, $F_{bi}$, and $F_{ti}$ are the suspension spring force, suspension damping force, and tire vertical force respectively at wheel i, and $m_w$ is the unsprung mass of the wheel. The rotational motion of each wheel is described with only a first order differential equation for its acceleration since tire angular displacement is not of interest for this effort. This acceleration is given by the following equation:

$$\omega_i' = T_i - \left(F_{ti} - R_{res}\right) R_{rad} / J_\omega \quad (14)$$

where $\omega_t$ is the angular velocity of wheel i, $T_i$ is the input torque to wheel i, and $R_{res}$, $R_{rad}$, and $J_\omega$ are constants representing the tire rolling resistance, rolling radius, and rotational moment of inertia of the tire-wheel assembly.

Several supporting equations are also required in the solution of the preceding differential equations. The total suspension force at each wheel referenced in (5) is given by:

$$F_{si} = F_{ki} + F_{bi} \quad (15)$$

and the equations for suspension spring and damping forces are respectively:

$$F_{ki} = k_i \left(Z_{cg} - L_{\theta i}\theta - L_{\phi i}\phi - Z_{ti}\right) \quad (16)$$

$$F_{bi} = b_i \left(Z_{cg}' - L_{\theta i}\theta' - L_{\phi i}\phi' - Z_{ti}'\right) \quad (17)$$

where $k_i$ and $b_i$ are the suspension spring and damping rates for wheel position i (note these need not be linear functions).

**Tire Model**

The tire provides the input and disturbances to the vehicle and for the skid-steer vehicle is probably the weakest part of the vehicle model. The drive and braking torques on the wheel provide input to the tire angular acceleration (as described earlier), but the representation of the interaction forces between the tire and the ground are not as accurately described. Various three-dimensional tire models have been developed based on experimental data [13]. These models, however, have been extrapolated from steady state tire test data and do not include adequate resolution at high longitudinal speed ratio and side slip values. Thus the tire models developed are quite adequate for conventionally steered vehicles, but do not extrapolate well to the conditions experienced with skid-steering maneuvers.

The tire model incorporated in the MATLAB skid-steer model represents tire forces in the global ground plane x-y coordinate system, as well as in the vertical direction. The vertical tire forces are modeled as the result of a linear spring representing a tire deflected vertically by a non-yielding ground (note tire damping could be easily added but is rather negligible for flat surface operation). This tire compressive force is given by the equation:

$$F_{ti} = k_t (Z_{gi} - Z_{ti}) \tag{18}$$

where $k_t$ is the tire spring coefficient, and $Z_{ti}$ and $Z_{gi}$ are the vertical positions of the tire center and tire-ground contact point for wheel i.

The tire forces in the ground plane are the result of tire longitudinal slip and tire side slip. The MATLAB model employs a sliding friction based representation of these forces and the lateral and longitudinal friction coefficients can be independently specified. The longitudinal force depends on tire vertical force and speed ratio. The effective coefficient of friction governing the longitudinal force can be input as any piecewise linear function of tire speed ratio (or longitudinal slip) similar to that shown in Figure 1 for the DADS tire model. The longitudinal tire force is defined as the ground reaction force in the direction the tire is oriented and is applied to the tire at the tire-ground contact point.

The lateral tire force, $F_{ilat}$, is determined as a linear function of individual tire vertical load and tire side slip angle. This is given by the following equation:

$$F_{ilat} = C_{lat} F_{ti} \theta_{ssi} \tag{19}$$

where $C_{lat}$ is the tire lateral stiffness or cornering coefficient, and $\theta_{ssi}$ is the side slip angle for wheel i.

The lateral force is also applied to the tire at the tire-ground contact point, but the lateral force is applied perpendicular to the plane of rotation of the tire. Since this vehicle model assumes that the tires are aligned with the major vehicle axes, the tire lateral and longitudinal forces are also chassis lateral and longitudinal forces.

## MODEL VERIFICATION AND VALIDATION EFFORTS

The final objective of developing these skid-steer models is to be able to use them to predict skid-steer turning performance and requirements and to subsequently assist in developing appropriate skid-steer control systems for implementation on future vehicles. The ultimate value and success of such an endeavor will depend greatly upon the accuracy and sensitivity of these models to the parameters of interest in the proposed wheeled vehicle skid-steer systems. With this in mind, a model verification and validation plan was undertaken. The validation effort has unfortunately to date been quite limited. Test data on skid steer vehicles is very sketchy and is almost nonexistent for higher speed operation. Even the tire data for high speed ratio and sideslip values is simply not available. Efforts are being pursued to obtain additional tire test data and to obtain a vehicle that can be utilized to obtain some limited skid-steer measurements.

The lack of sufficient test data placed additional emphasis on the development of a series of model verification simulations. These simulations were designed to isolate individual modes of the model in order to obtain an intuitive feel of the proper operation of the model. The series of runs then progressed to the execution of simple turning maneuvers to more fully verify the vehicle model.

Numerous simulations were conducted with both the DADS and the MATLAB models for verification purposes and to compare the qualitative results of the two systems. The two models both represented 4x4 vehicles with all non-steerable wheels. The DADS model represented a lightweight LAV derivative whereas the MATLAB model was meant to closely represent the Army's HMMWV. The two vehicles were still quite different in weight as can be seen from the vehicle characteristics shown in Table 1.

| Model parameter | DADS Concept | HMMWV | Units |
|---|---|---|---|
| GVW | 15200. | 6800. | lbs. |
| Unsprung weight | 1200. | 800. | lbs. |
| Pitch Inertia | 11876. | 4390. | lb-sec$^2$-ft |
| Roll Inertia | 2792. | 1500. | lb-sec$^2$-ft |
| Yaw Inertia | 13002. | 6000. | lb-sec$^2$-ft |
| Wheel base | 11.58 | 10.82 | ft |
| Track width | 7.17 | 7.00 | ft |
| cg from front axle | 5.83 | 5.02 | ft |
| Tire lateral | 467. | | lbs/deg |

The simulations reported here for both DADS and MATLAB were initiated with equal torque applied across each axle. This caused the vehicle to initially travel in a straight line. At a given time the torque inputs to the various wheels were varied in a predetermined manner to cause a particular vehicle maneuver to be executed. Lane change and circular maneuvers were simulated but the circular maneuvers seemed to provide the more interesting arena for parameter variation results, and so the following discussion is limited to these runs.

**DADS Model Simulation Results**

Figure 5 displays several results obtained from running the simulation with a large drive torque applied to the right side wheels, while a simultaneous large braking torque was applied to the left side wheels. The vehicle had an initial velocity of 20 mph and for the first 5 seconds had just enough torque to overcome the rolling resistance. After 5 seconds, a torque of 2000 ft-lbs was applied to the two right side wheels while a torque of –1687 ft-lbs was applied to the left side. This unbalanced torque application was to cause the vehicle to begin turning to the left in a nearly circular pattern as shown in Figure 5a. Figure 5b shows a corresponding increase in vehicle velocity as the maneuver is continued.

Figures 5c and 5d show the tire side slip for the front left and rear left tires during this simulation. The right front and right rear tires track their left hand counterparts quite closely and are not shown here. It should be noted that as the vehicle velocity changes, the tire side slip angles also change and in fact the side slip of the front tire actually changes sign during this maneuver. It is also worth noting that in general, the side-slip angles of the front and rear tires are definitely not equal in magnitude and opposite in sign as has often been assumed in previous modeling efforts. Although, there may be a particular speed and turning radius at which this could occur. Figures 5e and 5f show the corresponding lateral forces for the left side tires.

Figure 6 documents a similar DADS simulation, but one where the total drive and braking torques during the turning maneuver have been adjusted to provide a nearly constant velocity turn. Figure 6a and 6b demonstrate that a more constant vehicle path and velocity have been achieved. Figure 6c and 6d reflect the chassis roll angle and lateral acceleration for this steady state maneuver. Figures 6e and 6f show the side slip angle time histories for the left side tires. When these latter two plots are compared to the changing angles in 5c and 5d, it becomes clear that the side slip was in fact changing primarily due to the changing vehicle velocity. One can also compute the centripetal acceleration based on a circular path of 165 ft radius (estimated from Figure 6a) at 20 mph and obtain a value of 5.2 ft/sec$^2$. This agrees closely with the steady state lateral acceleration shown in Figure 6d.

**MATLAB Simulation Results**

The MATLAB model of the HMMWV was developed from basics and therefore required a more detailed verification effort. Various test cases were devised to check the behavior of different vehicle motions independently. The results shown in Figure 7 are just such a case. Figure 7a shows the drive torque profile provided to each wheel. After 1.5 seconds, the drive torque was uniformly ramped up on all wheels to accelerate the vehicle in the forward direction. Figure 7b shows the resulting vehicle velocity response. Vehicle pitch motion and tire longitudinal behaviors were also observed to ensure the reasonableness of the model behavior. The maximum drive torque level was also adjusted to provide approximately the acceleration performance (in the 0-50 mph range) demonstrated by the hybrid HMMWV.

Providing an initial vehicle velocity of 20 ft/sec and just enough drive torque to maintain a straight-line course at that speed generated the results shown in Figure 8. The vehicle was given an initial heading angle of 0 degrees but an initial yaw angle of 2.8 degrees. This caused an initial side slip angle of 2.8 degrees for each tire and corresponding lateral side forces on the tires. Figure 8a shows the vehicle heading and yaw responses while Figure 8b contains plots of the lateral forces on the right side tires.

The simulation results shown in Figure 9 for the MATLAB model are similar to those for the DADS model in Figure 7. In this case, however, the vehicle was simulated at a velocity of 40 ft/sec and the right side wheels were driven with a torque of 1000 ft-lbs while the left side wheels each received a braking torque of –840 ft-lbs. This resulted in a steady state circular vehicle path shown in Figure 9a. Figure 9b demonstrates the steady state behavior of the vehicle velocity and the right front tire angular velocity. Figure 9c presents the chassis roll motion response and Figure 9d gives the vehicle lateral and longitudinal acceleration time histories. If the centripetal (also the lateral in this case) acceleration is computed from a velocity of 40 ft/sec and a turning radius of 170 ft, the value of 9.4 ft/sec$^2$ is obtained. Again this agrees quite closely with the steady state value for lateral acceleration shown in Figure 9d.

Figure 9e shows the tire side slip angles for the two right side tires. Once again it should be noted that they are definitely not symmetrically positioned about zero. In fact for this particular condition, the front and rear right side tires both have a positive side slip angle. Figure 9f shows the chassis yaw and heading angles throughout this maneuver. It can be seen here that this particular simulation encompassed over two complete loops of the circular path.

The MATLAB simulation reported in Figure 10 was used to explore the tire model transient behavior more fully. The simulation lasted for only 5 seconds, which consisted of the normal 2 seconds of straight-line travel followed by a gentle left turn for the remaining 3 seconds. The vehicle speed was initialized at 20 ft/sec and the tire-cornering rate was one half of the nominal rate.

Figure 10a shows the vehicle path traversed and Figure 10b provides the input drive torque for each of the front axle wheels. Figures 10c and 10d show the front tire slip ratio and resulting tire angular velocity time histories. It can be seen from the difference in response of the left and right side tires that the vehicle is turning left and slowing down. Figure 10e records the transient to steady state progression of the lateral slip of the right side tires. Figure 10f shows the effect of the turning on the lateral velocity (in global coordinates) of the right side tire hubs. Figure 10g and 10h document the vehicle yaw and heading time histories for this maneuver.

The MATLAB simulation from which Figure 11 was generated provided a very modest turning torque and applied that torque for only 2 seconds before returning to the equally applied drive torques required to simply sustain vehicle velocity. Once again the tire cornering stiffness was set at one half its nominal value. Figure 11a documents the input torque profiles for the front wheels (the rear were once again driven identically). Figure 11b shows the chassis pitch and roll response to this 2-second duration left turn correction maneuver. The vehicle yaw and heading angles are plotted in Figure 11c. The vehicle begins to yaw before it changes direction (i.e. heading). Once the unbalanced turning torques are terminated at 4 seconds, the vehicle once again proceeds in a straight line but at a slightly modified direction (by 1.6 degrees). Figure 11d records the side slip of the right side tires during this simulation.

## FUTURE MODEL PLANS AND USAGE

Two areas will be actively pursued in the coming months as the use of these models is contemplated for the development of differential torque steer controllers. The first is to obtain representative vehicle test data that can be used to evaluate the models capabilities and weaknesses. There are two separate 4x4 electric drive vehicles that may become available for such testing later this year.

The second issue concerns the tire model and tire data. Attempts to perform pivot steer maneuvers with both models seem to generate excessively slow vehicle yaw rates. It is conjectured that the combined high side slip and longitudinal speed ratios are not adequately modeled for this situation. Tire data is generally not available for this combined high slip situation.

Tire test data is always scarce and when it is available it is generated for steady state, small side slip scenarios. When a differential torque steer (or skid-steer) vehicle executes a pivot steer or very short radius turn, the tire sideslip angles quickly exceed the normal range of tire test data. Since the tire model is based on experimental data, the model itself is very suspect for large side slip situations. The effective tire ground plane forces for the combined large side slip and longitudinal slip situation may also require further refinement. It is indicated in [7] that there may be considerable more tire force attenuation in these situations than indicated by the friction ellipse approach. Possibilities are being explored to obtain more extensive tire test data for a representative tire.

The models will be used to carry out parameter sensitivity studies on the differential torque steered vehicles. Turning capabilities and yaw motion sensitivity will be evaluated for a variety of vehicle maneuvers. It is envisioned that subsequently one of the models will be used in the design and evaluation of a differential torque steering controller before installation and testing on an electric drive, non-steerable wheel vehicle testbed.

## SUMMARY AND CONCLUSIONS

The development and verification of two independent models for differential torque steer vehicles serves as a prerequisite to the development of appropriate steering algorithms for such systems. These models have been shown to be sensitive to a wide variety of vehicle design parameters but will require further refinement and validation as the differential torque steer systems evolve. With the development of a variety of different electrically driven wheeled demonstration vehicles, the potential flexibility and utility of differential torque steer systems has greatly increased over that of mechanically driven systems. It now seems quite possible, with the use of modern digital control technology, to develop a differential torque steer vehicle that would handle quite adequately even at higher operating speeds. It is envisioned that the steering controller for such a vehicle would include capability similar to that in the anti-skid dynamic yaw control systems currently being demonstrated on a variety of automobiles. The selective torque application dictated by such a controller would prevent the operator from oversteering and skidding out the vehicle, while allowing the maximum turning capability of the system to be utilized whenever it is called for.

## REFERENCES

1. A.R. Kovnat, "Contemporary Problems in Tracked Vehicle Steering," TARDEC Technical Report No. 13726, US Army TACOM, Warren, Michigan, June 1997.

2. L. Mangialardi, "Study of the Horizontal Plane Motion of a Skid-Steering Vehicle," Proceedings of 7th International Conference of ISTVS, pp. 1448-1472, Calgary, Alberta, Canada, 1981.

3. A. Gentile and L. Mangialardi, "Behavior of a Non-Conventional Transmission and Skid-Steering Vehicle," Proceedings of 19th International FISITA Congress: Energy Mobility, Melbourne, Australia, SAEA Paper No. 82090, November 1982.

4. A. Gentile and L. Mangialardi, "Dynamic Steering Multiaxle Vehicles: Influence on Axle-Numbers," Proceedings of 20th International FISITA Congress: The Automotive Future, Vienna, Austria, SAE Report No. 845056, May 1984.

5. A.P. Creedy, "Skid Steering of Wheeled and Tracked Vehicles – Analysis with Coulomb Friction Assumptions," Engineering Development Establishment Report AR No 002.715, Victoria, Australia, December 1984.

6. I. Schmid and W. Tomaske, "Power and Torque Requirements for Skid Steering Vehicles," Proceedings of ISTVS Conference on Off-Road Vehicles, FISITA 92, London, U.K., pp. 216-230, June 1992.

7. C. Renou and S. Chavant, "A Computer Simulation Model for Skid-Steering of Non-Directed Wheeled Vehicles," Proceedings of 11th International Conference of ISTVS, pp. 398-407, Lake Tahoe, Nevada, 1993.

8. B. Durand, J.L. Favero, and C. Renou, "MODIX, A 8x8 Steering Research Vehicle," Proceedings of International Conference of ISTVS, pp. 487-495, Italy, October 1997.

9. DADS 8.0 Reference Manual, Volume 1, Computer Aided Design Software, Inc., Coralville, IA, November 1995.

10. D. Hanselman and B. Littlefield, MATLAB Version 5 User's Guide, The Math Works, Inc., Prentice Hall, Upper Saddle River, NJ, 1997.

11. T.D. Gillespie, Fundamentals of Vehicle Dynamics, SAE, Warrendale, PA, 1992.

12. W.F. Milliken and D.L. Milliken, Race Car Vehicle Dynamics, SAE, Warrendale, PA, 1995.

13. J.C. Dixon, Tires, Suspension and Handling, Second Edition, SAE, Warrendale, PA, 1996.

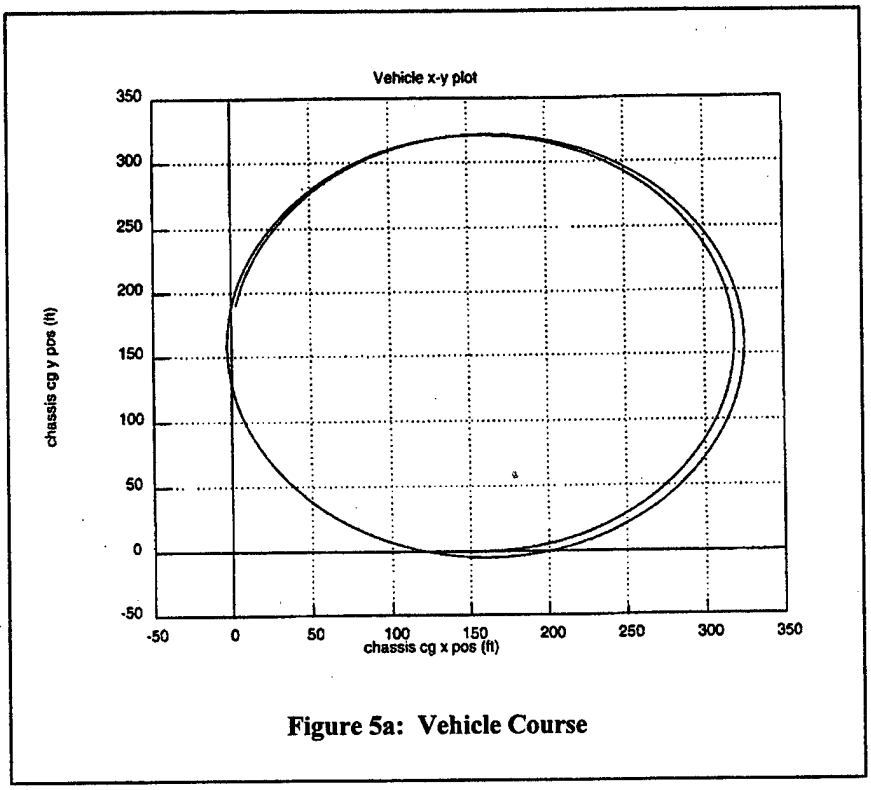


**Figure 5a: Vehicle Course**

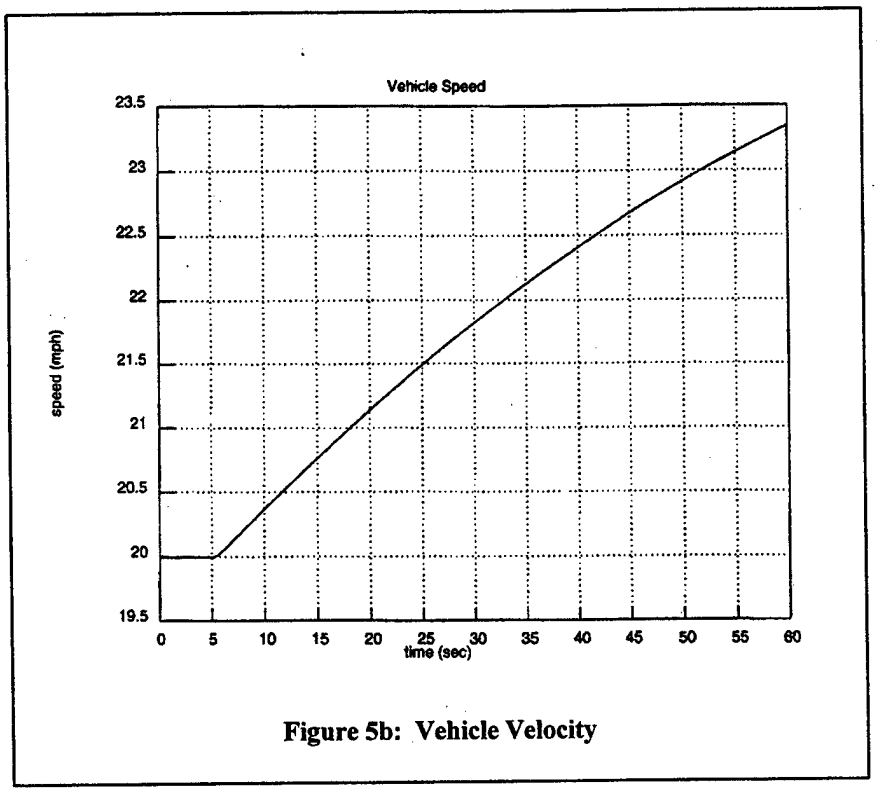


**Figure 5b: Vehicle Velocity**

Figures 5a and 5b. DADS simulation results with right side drive torques at 2000 ft-lb and left side at -1687 ft-lb. a) near circular vehicle course; b) vehicle velocity time history during maneuver.

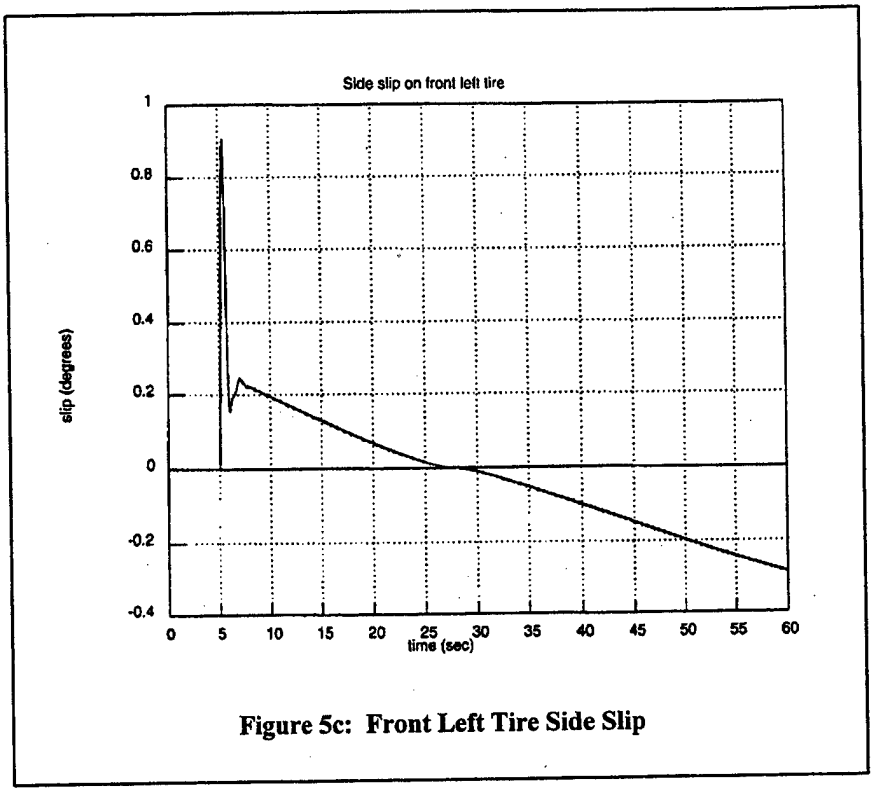


**Figure 5c: Front Left Tire Side Slip**

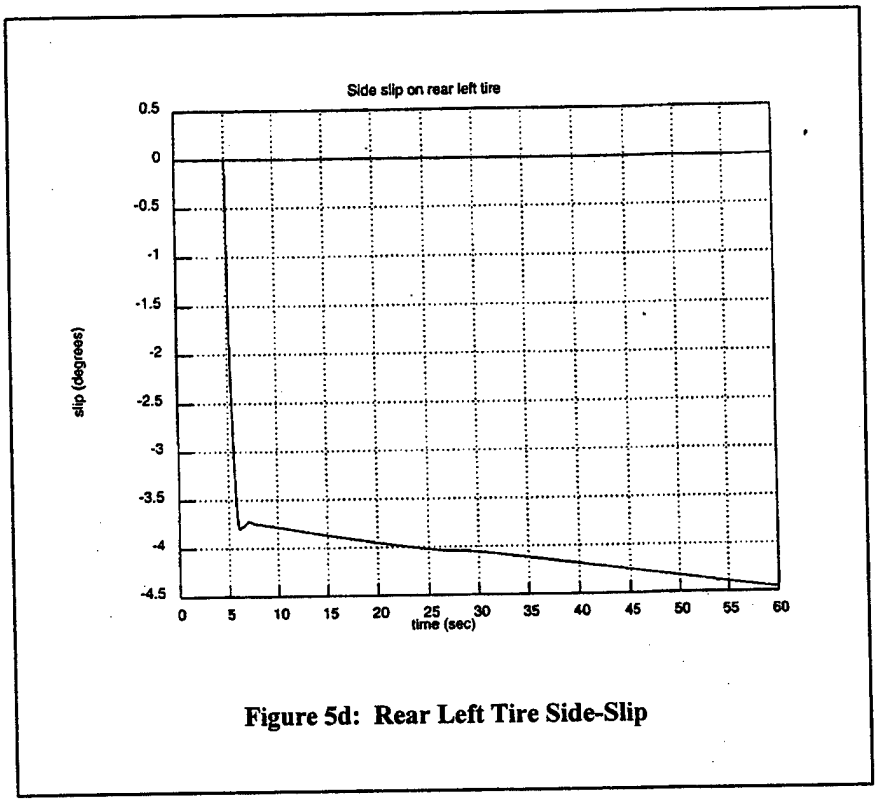


**Figure 5d: Rear Left Tire Side-Slip**

Figures 5c and 5d. DADS simulation results with right side drive torques at 2000 ft-lb and left side at -1687 ft-lb. c) front left tire side slip d) rear left tire side slip.

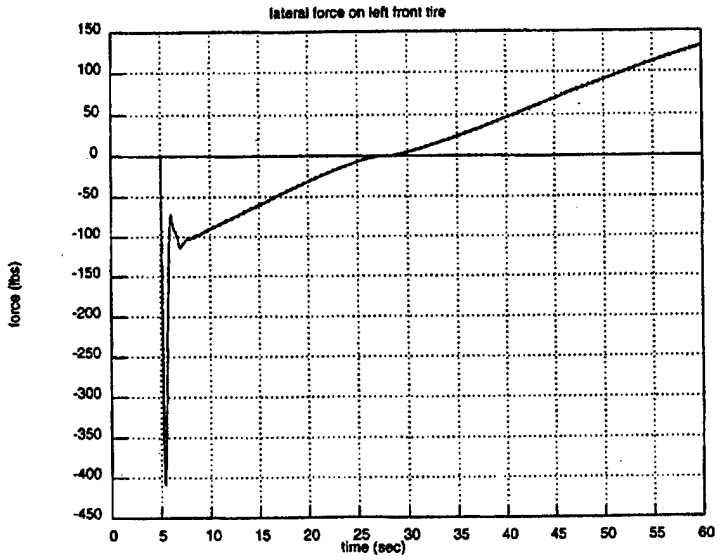


**Figure 5e: Left Front Tire Lateral Force**

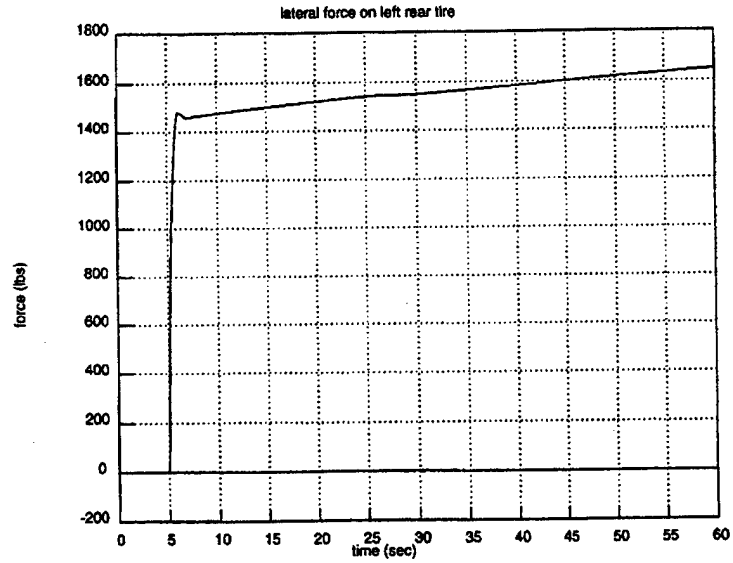


**Figure 5f: Rear Left Tire Lateral Force**

Figures 5e and 5f. DADS simulation results with right side drive torques at 2000 ft-lb and left side at -1687 ft-lb. e) front left tire lateral force f) rear left tire lateral force.

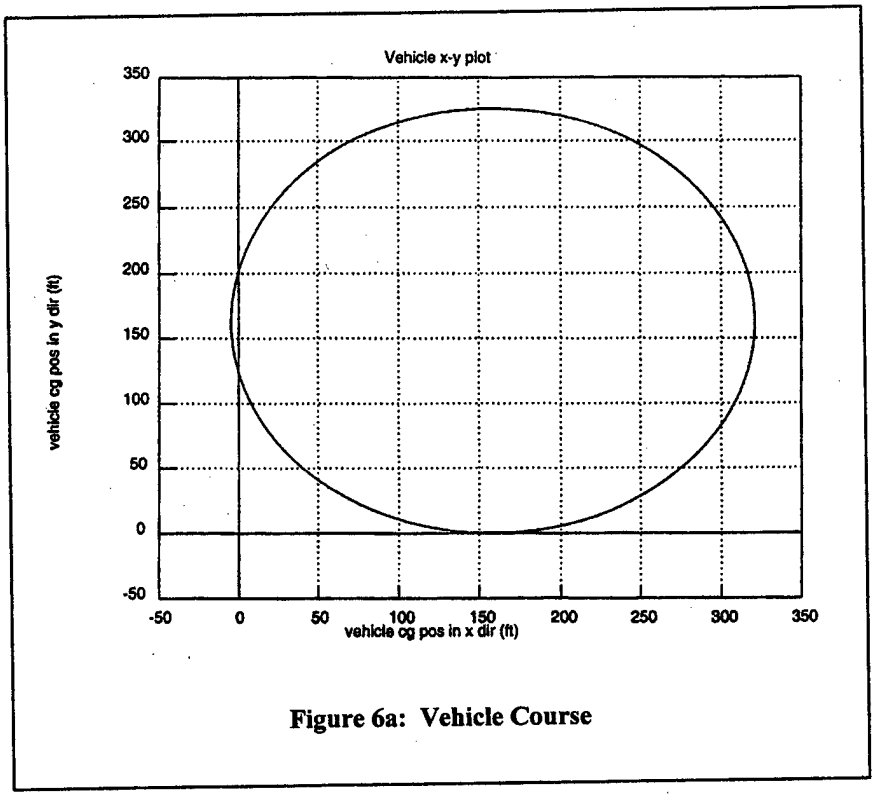


**Figure 6a: Vehicle Course**

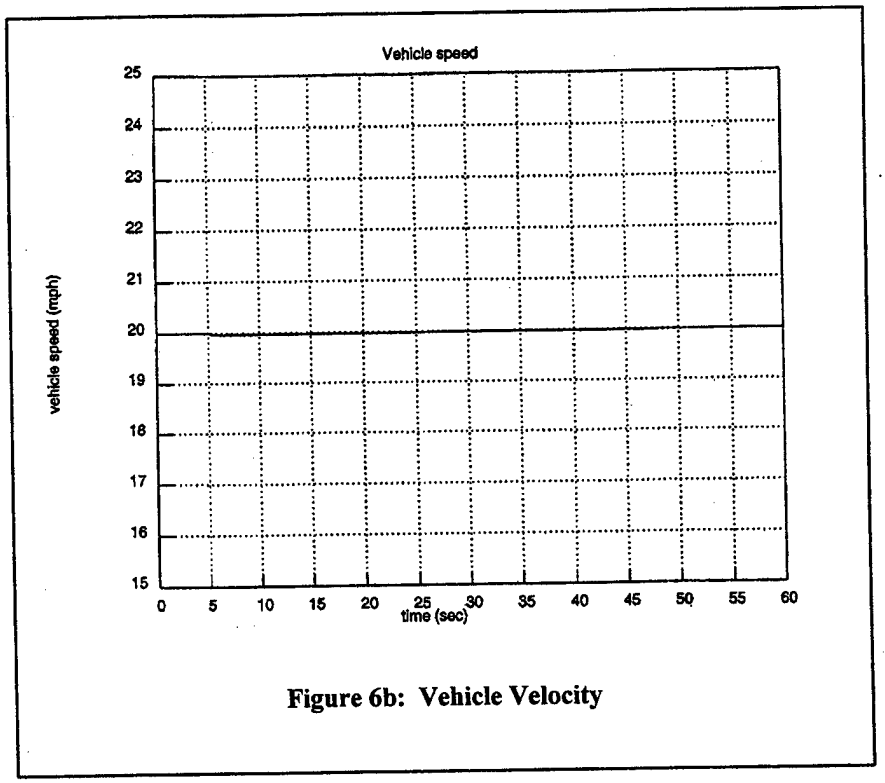


**Figure 6b: Vehicle Velocity**

Figures 6a and 6b. DADS simulation results with right side drive torques at 1956 ft-lb and left side at -1687 ft-lb. a) near circular vehicle course; b) vehicle velocity time history during maneuver.

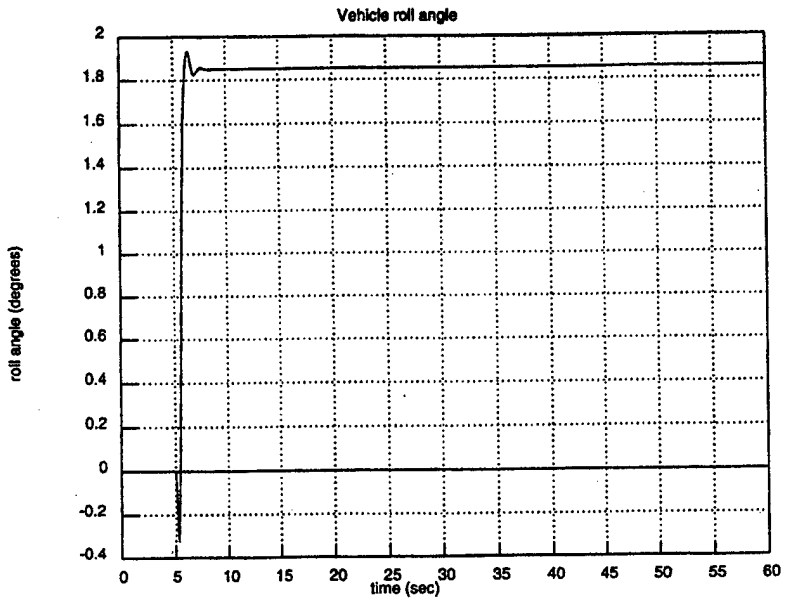


**Figure 6c: Vehicle Roll Angle**

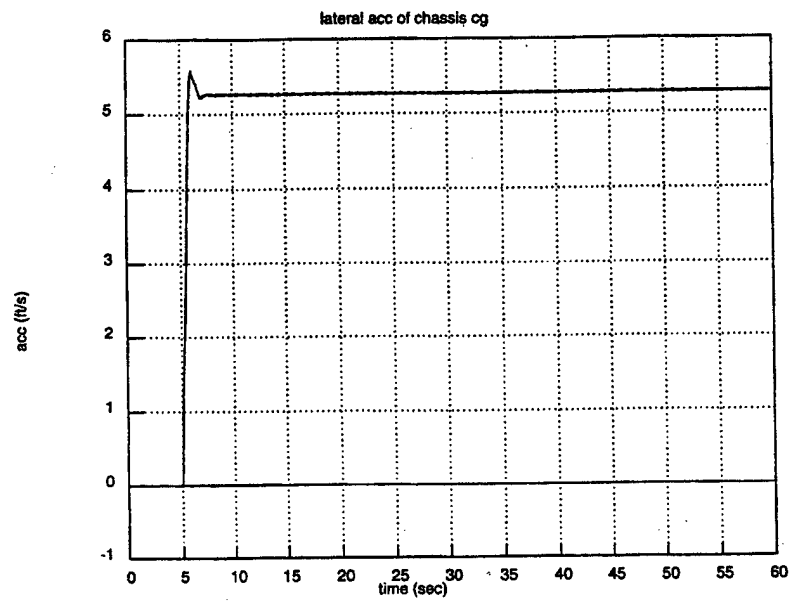


**Figure 6d: Vehicle Lateral Acceleration**

Figures 6c and 6d. DADS simulation results with right side drive torques at 1956 ft-lb and left side at -1687 ft-lb. c) chassis roll angle; d) vehicle lateral acceleration time history during maneuver.

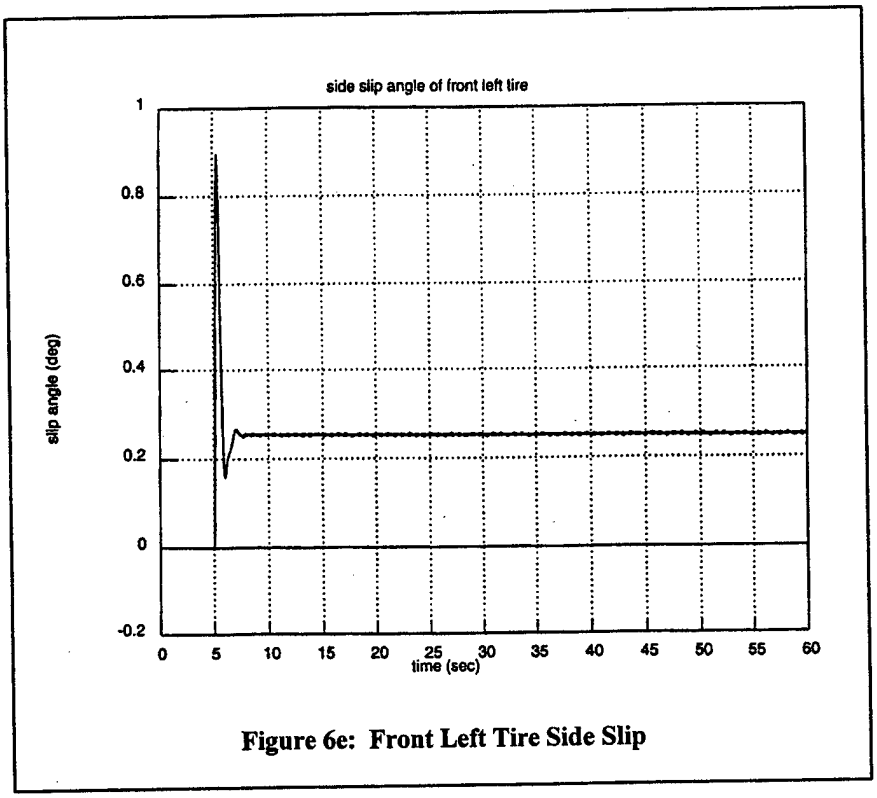


**Figure 6e: Front Left Tire Side Slip**

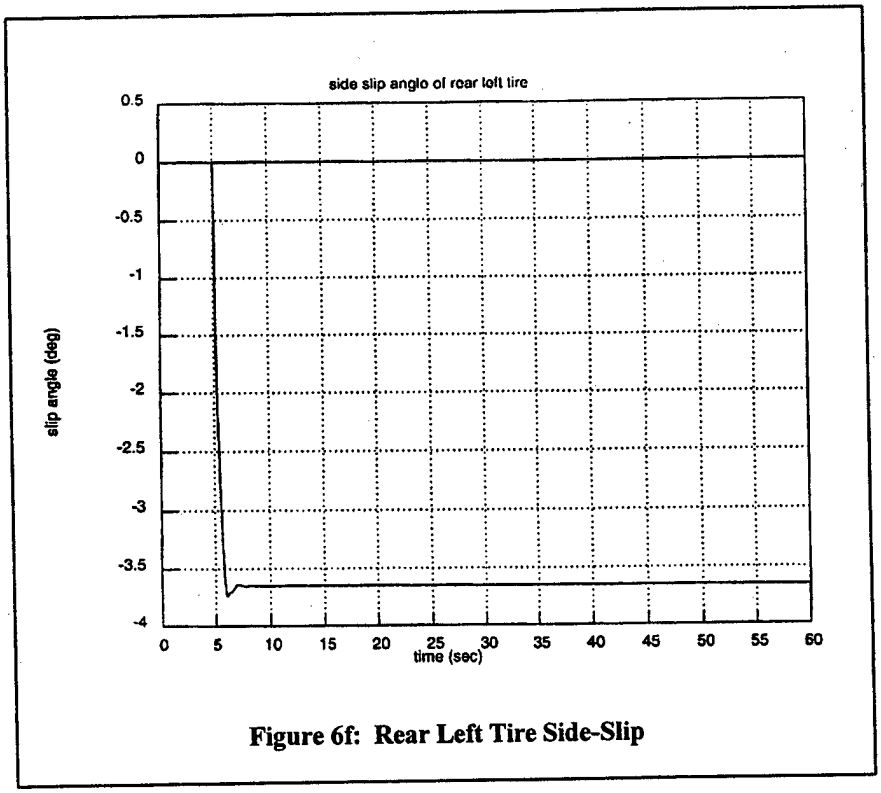


**Figure 6f: Rear Left Tire Side-Slip**

Figures 6e and 6f. DADS simulation results with right side drive torques at 1956 ft-lb and left side at -1687 ft-lb. e) front left tire side slip f) rear left tire side slip.

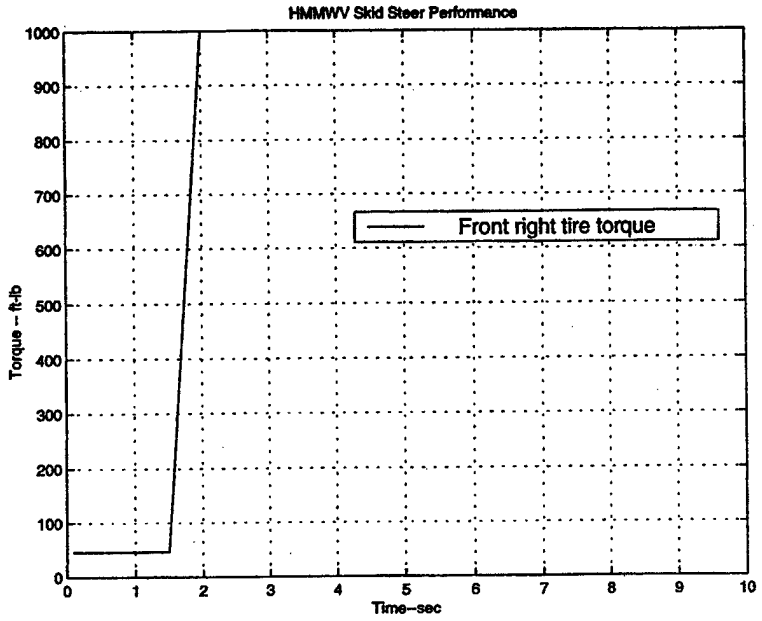


**Figure 7a: Torque On All Wheels**

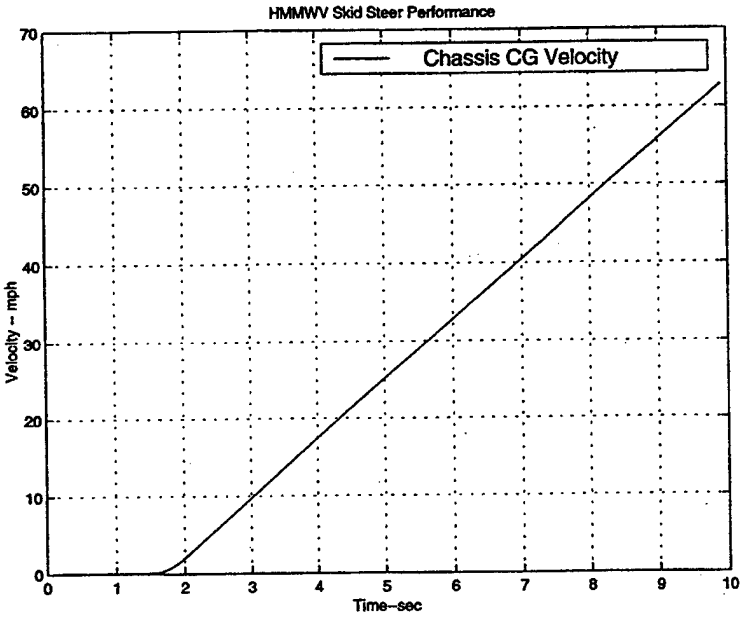


**Figure 7b: Vehicle Velocity**

Figures 7a and 7b. Matlab simulation results with equal acceleration torque profile on all wheels. a) torque time history for all wheels b) vehicle velocity response.

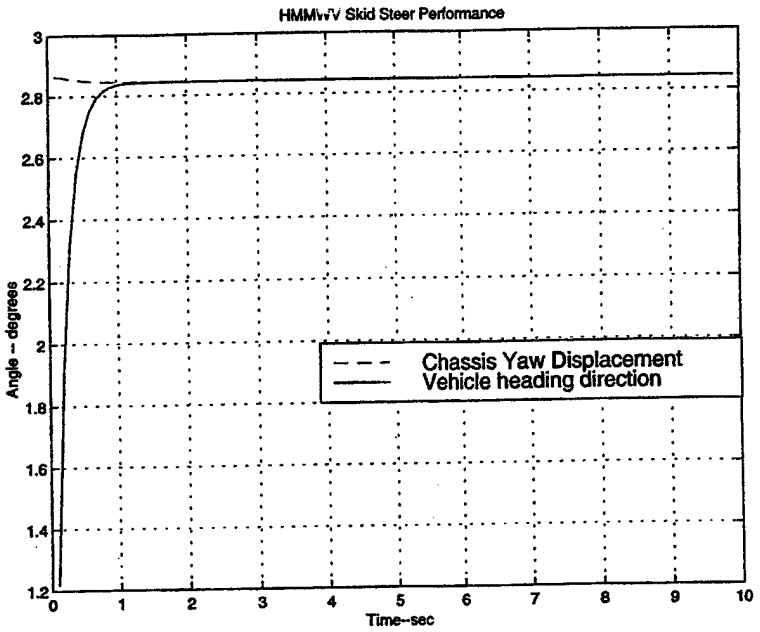


**Figure 8a: Vehicle Yaw and Heading**

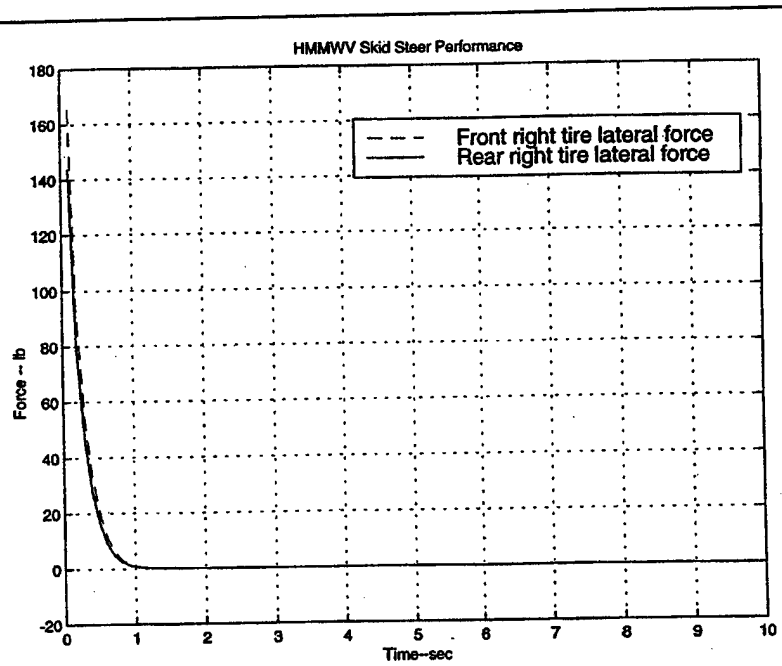


**Figure 8b: Vehicle Right Side Tire Lateral Forces**

Figures 8a and 8b. Matlab simulation results with equal speed sustaining torque profile on all wheels, initial velocity of 20 ft/sec, and an initial yaw angle of 2.8°. a) chassis yaw and heading time responses; b) right side tire lateral forces.

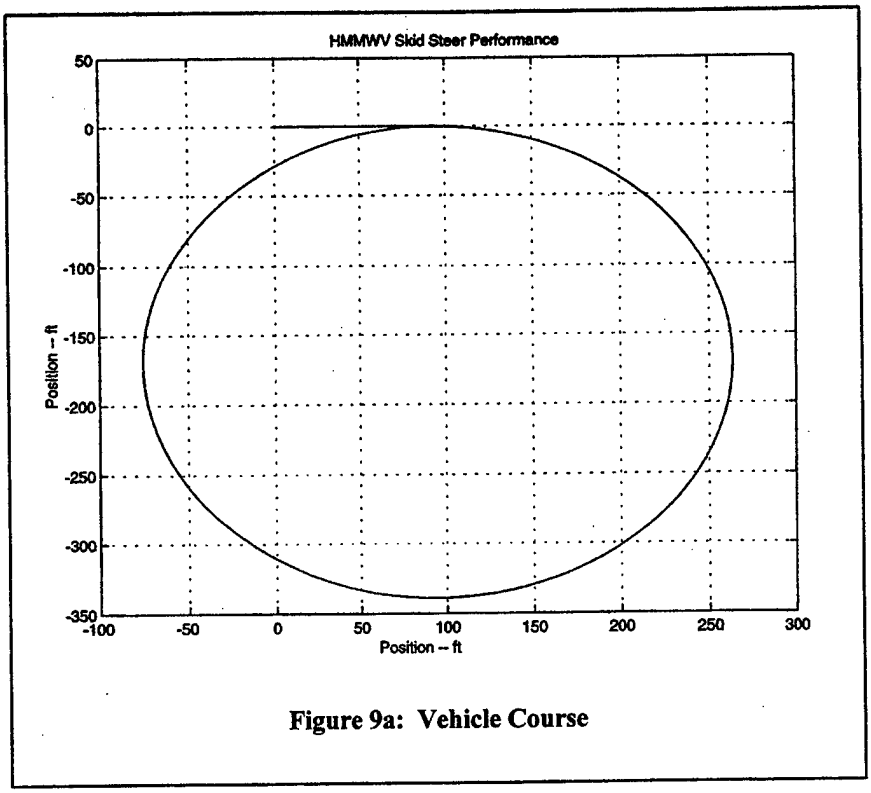


**Figure 9a: Vehicle Course**

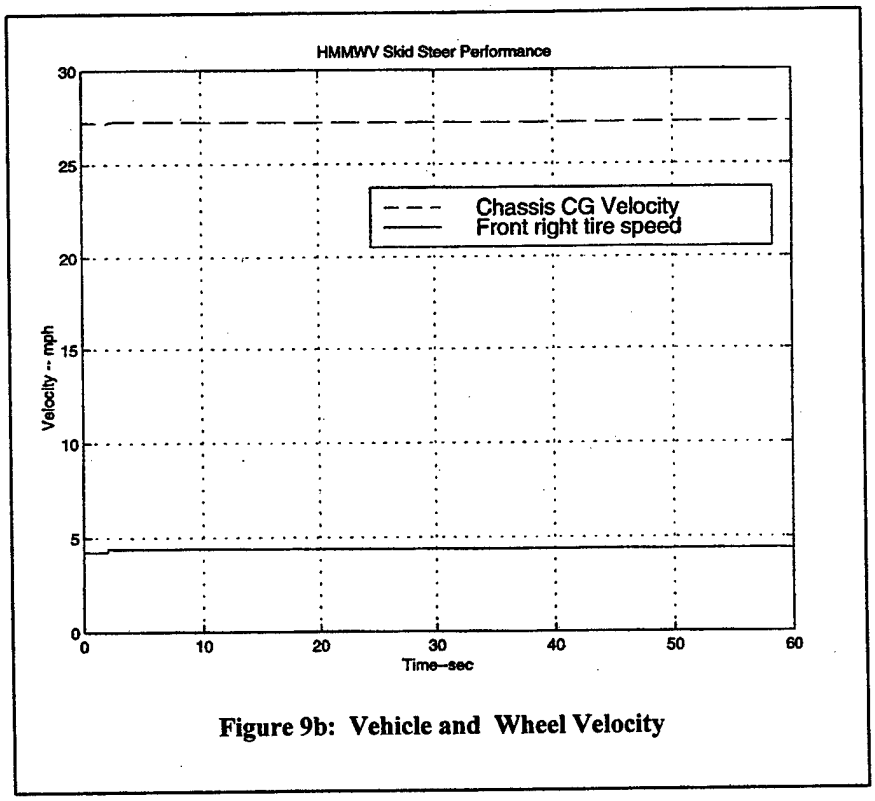


**Figure 9b: Vehicle and Wheel Velocity**

Figures 9a and 9b. Matlab simulation results with right side drive torque of 1000 ft-lbs and left side braking torques of –840 ft-lbs on each wheel. a) circular path of vehicle maneuver; b) vehicle velocity and front right tire angular velocity.

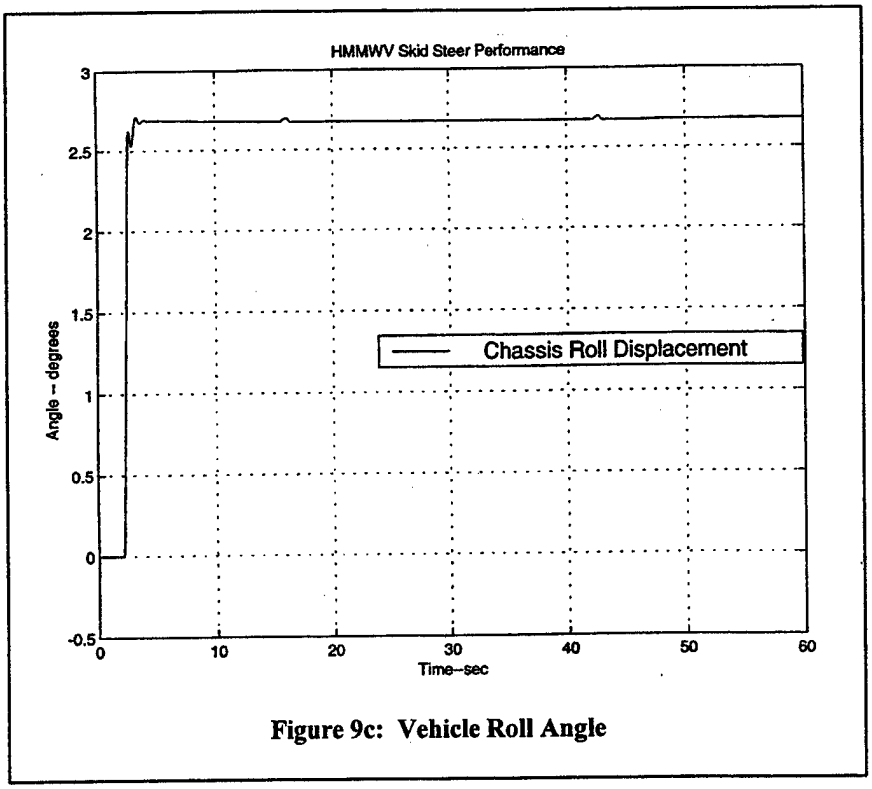


**Figure 9c: Vehicle Roll Angle**

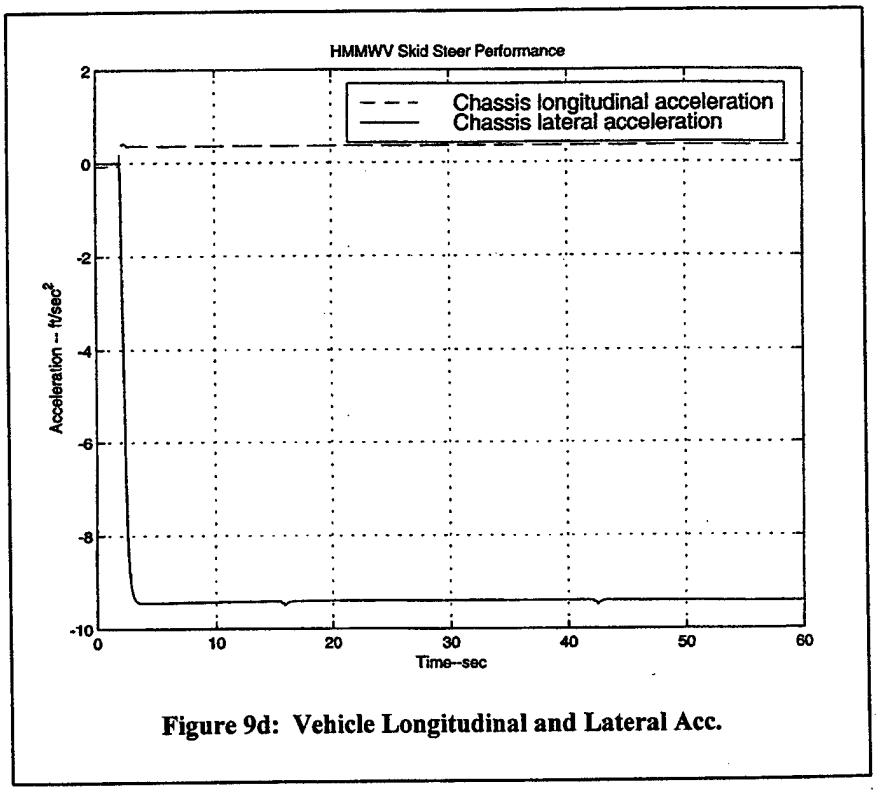


**Figure 9d: Vehicle Longitudinal and Lateral Acc.**

Figures 9c and 9d. Matlab simulation results with right side drive torque of 1000 ft-lbs and left side braking torques of –840 ft-lbs on each wheel. c) chassis roll motion; d) chassis longitudinal and lateral accelerations.

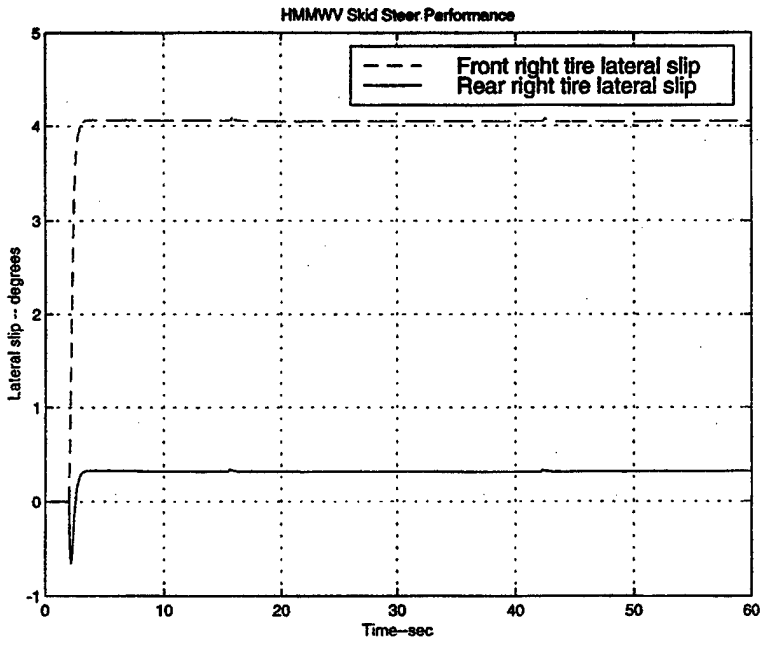


**Figure 9e: Right Side Tire Lateral Slip**

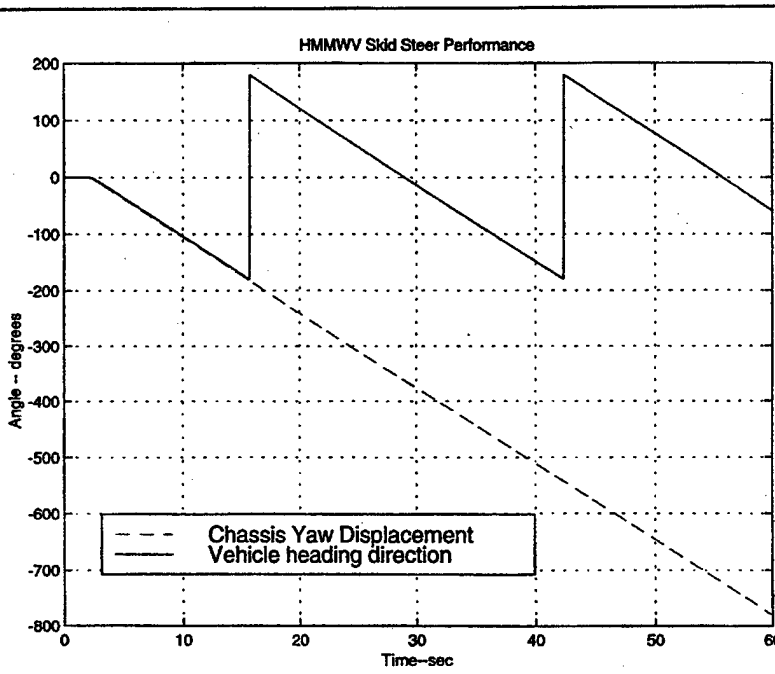


**Figure 9f: Side Slip Angles for Right Side Tires**

Figures 9e and 9f. Matlab simulation results with right side drive torque of 1000 ft-lbs and left side braking torques of –840 ft-lbs on each wheel. e) side slip angles for right side tires; f) vehicle yaw and heading responses for circular maneuver.

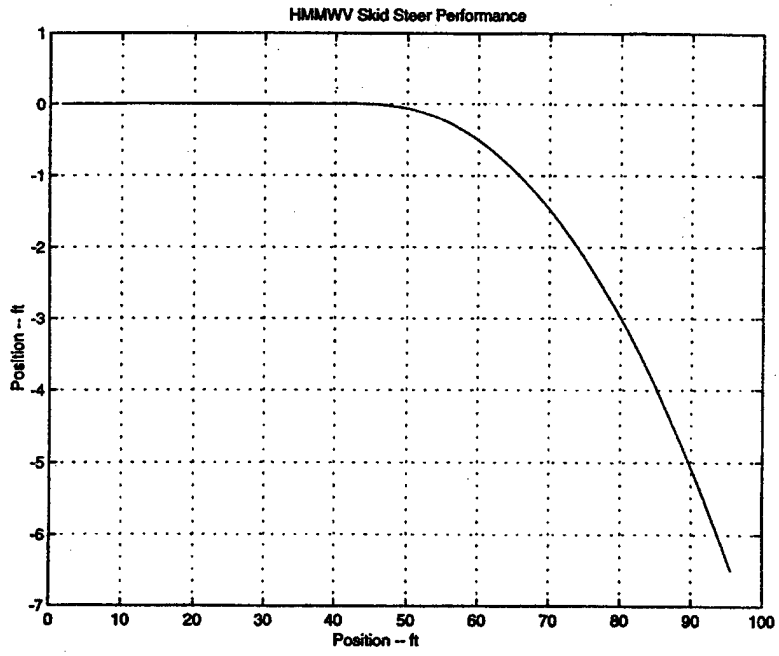


**Figure 10a: Vehicle Course**

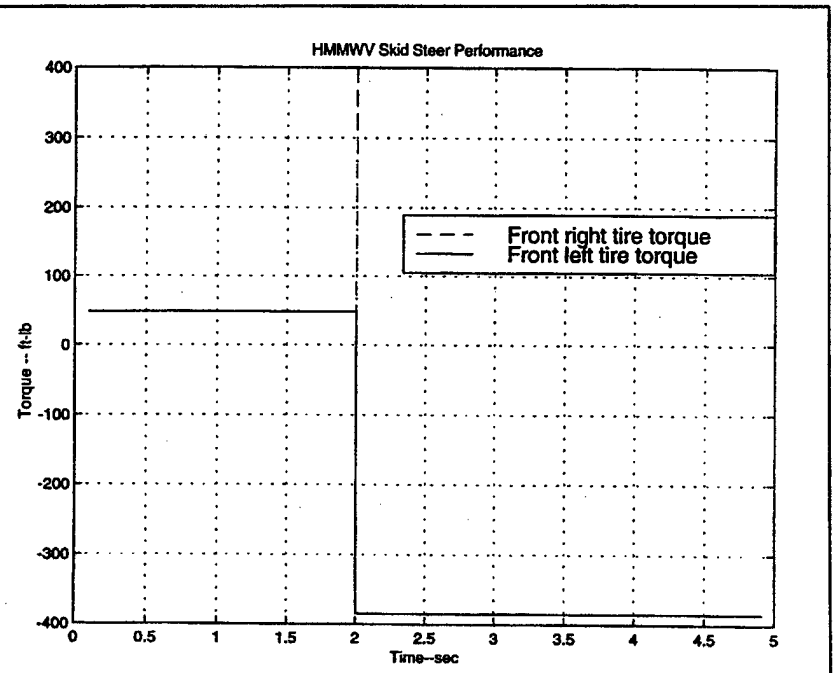


**Figure 10b: Vehicle Front Axle Input Torques**

Figures 10a and 10b. Matlab simulation results with right side drive torques of 400 ft-lbs and left side braking torques of –385 ft-lbs on each wheel and half the nominal tire cornering stiffness. a) path of vehicle maneuver; b) vehicle front axle input torques.

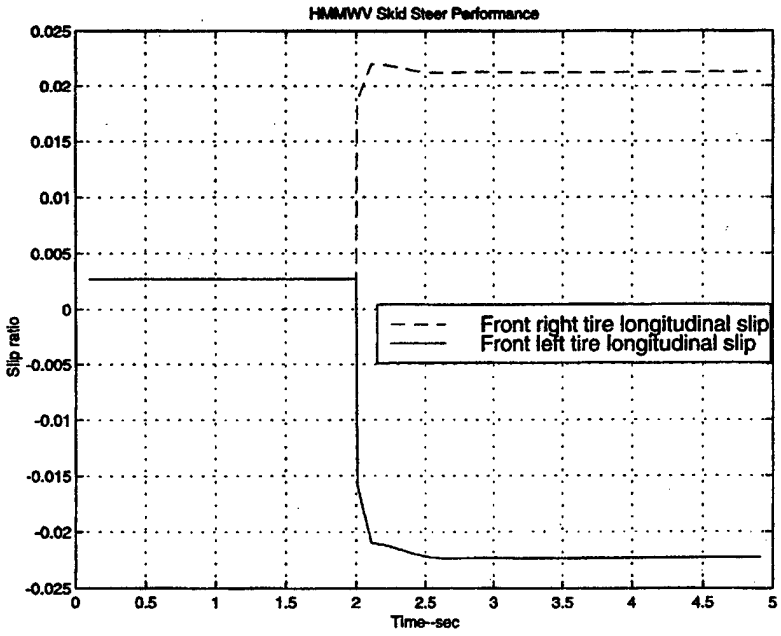


**Figure 10c: Front Axle Longitudinal Slip**

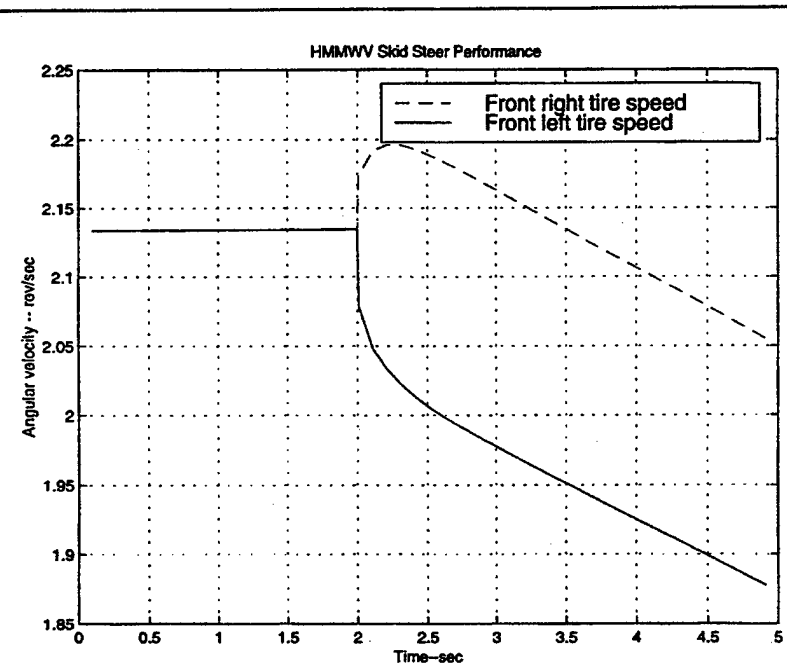


**Figure 10d: Front Axle Wheel Speeds**

Figures 10c and 10d. Matlab simulation results with right side drive torque of 400 ft-lbs and left side braking torques of –385 ft-lbs on each wheel and half the nominal tire cornering stiffness. c) front axle longitudinal slip responses; d) front axle wheel speeds.

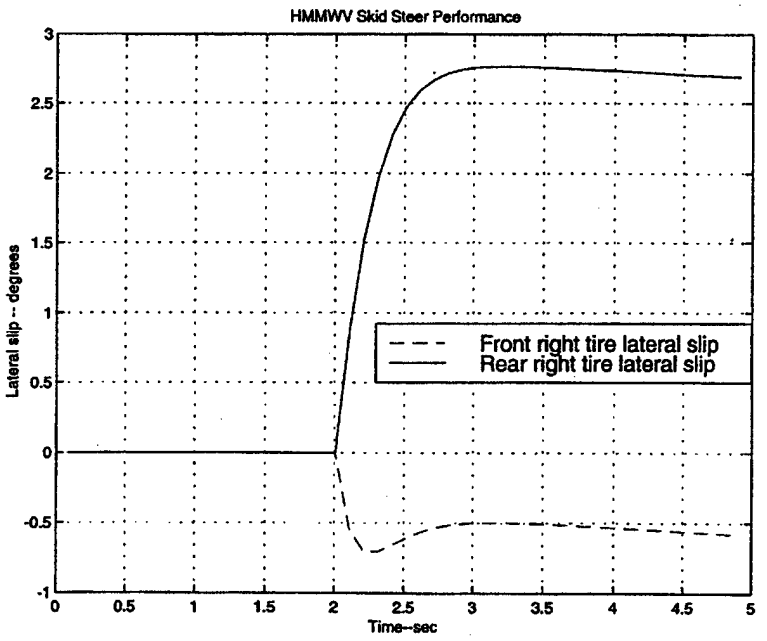


**Figure 10e: Front Axle Lateral Slip**

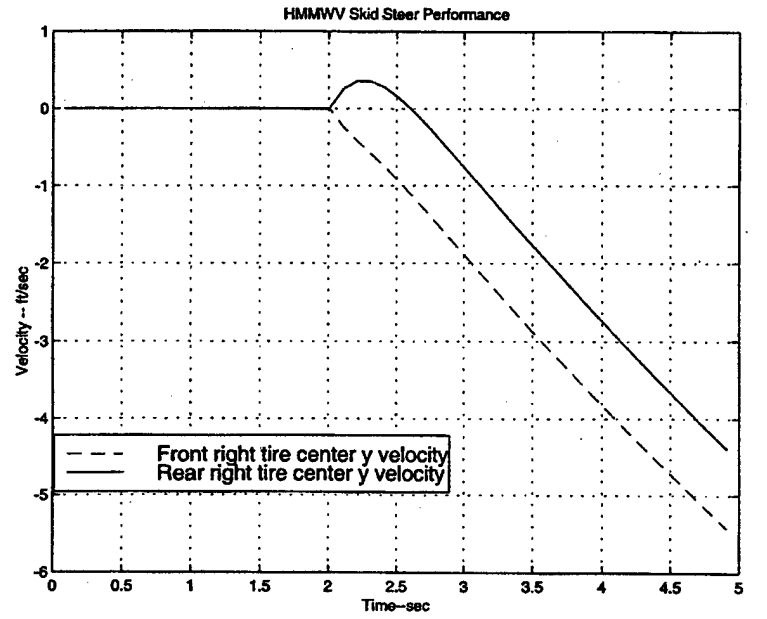


**Figure 10f: Front Wheel Global Y-Velocities**

Figures 10e and 10f. Matlab simulation results with right side drive torque of 400 ft-lbs and left side braking torques of –385 ft-lbs on each wheel and half the nominal tire cornering stiffness. e) front axle tire side-slip angles; f) front axle wheel hub global y-velocities.

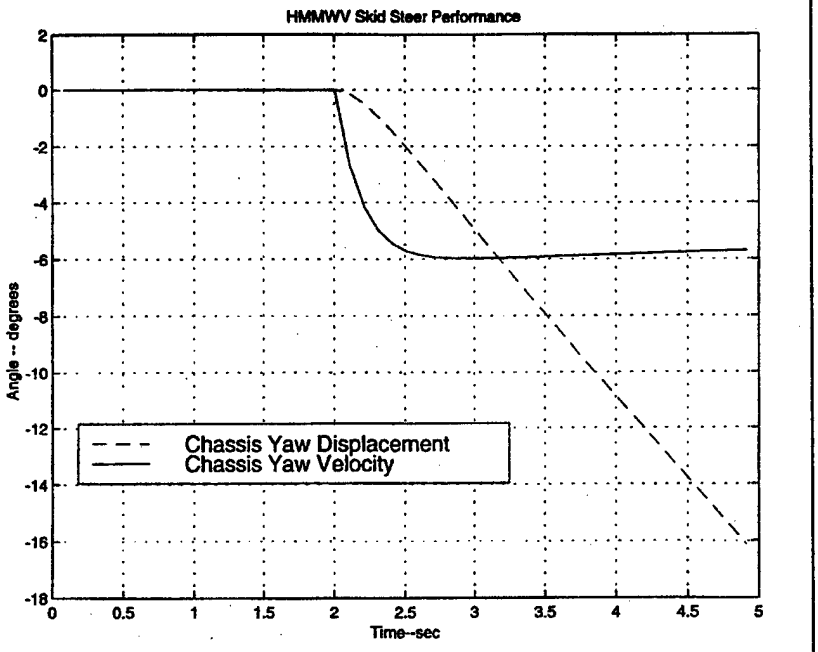


**Figure 10g: Vehicle Yaw Angle and Velocity**

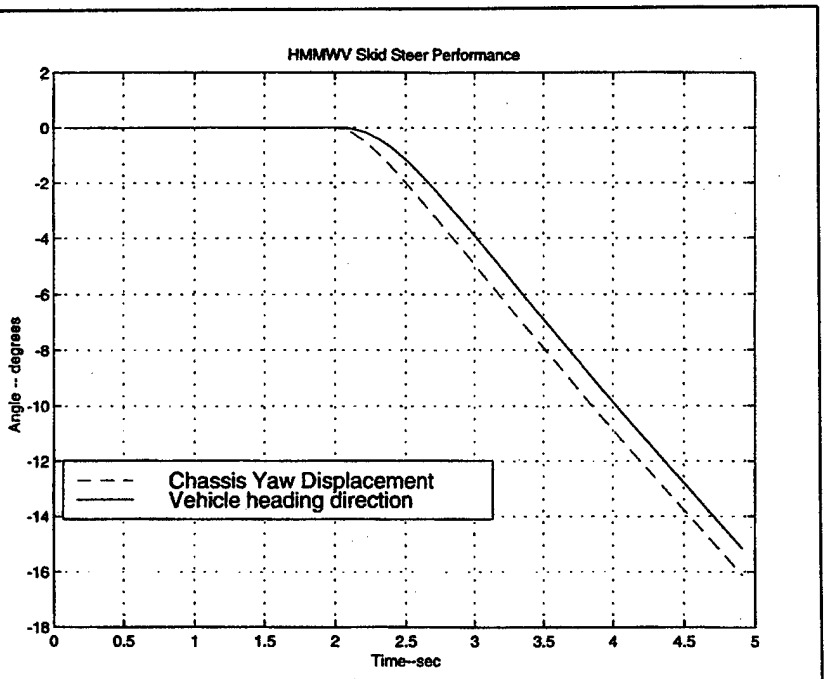


**Figure 10h: Chassis Yaw and Heading Angles**

Figures 10g and 10h. Matlab simulation results with right side drive torque of 400 ft-lbs and left side braking torques of –385 ft-lbs on each wheel and half the nominal tire cornering stiffness. g) vehicle yaw motion; b) chassis yaw and heading angles.

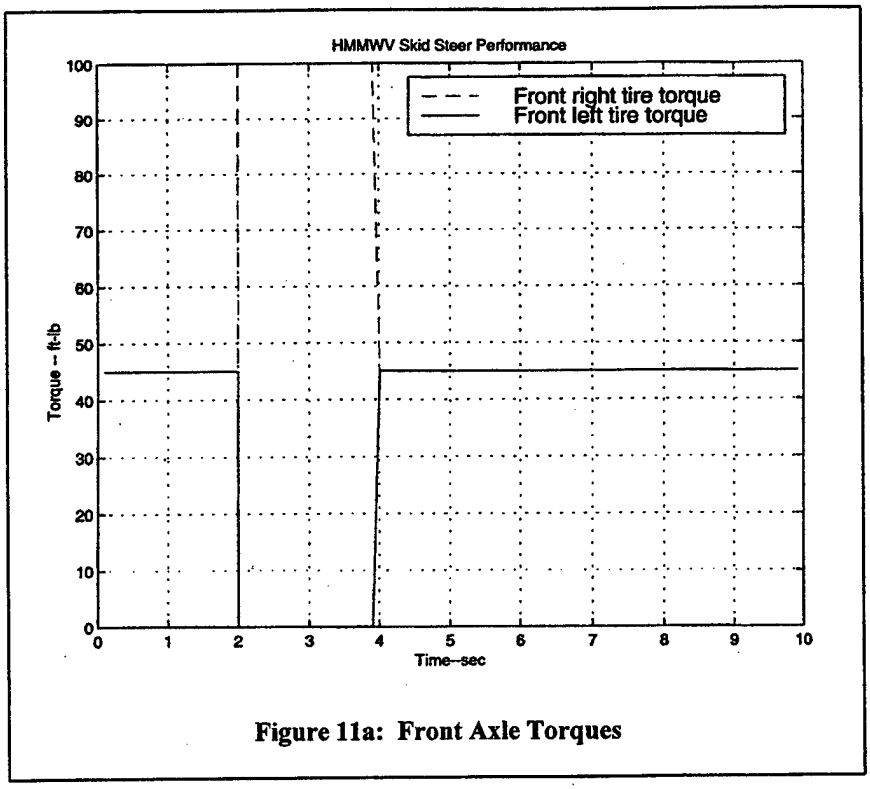


**Figure 11a: Front Axle Torques**

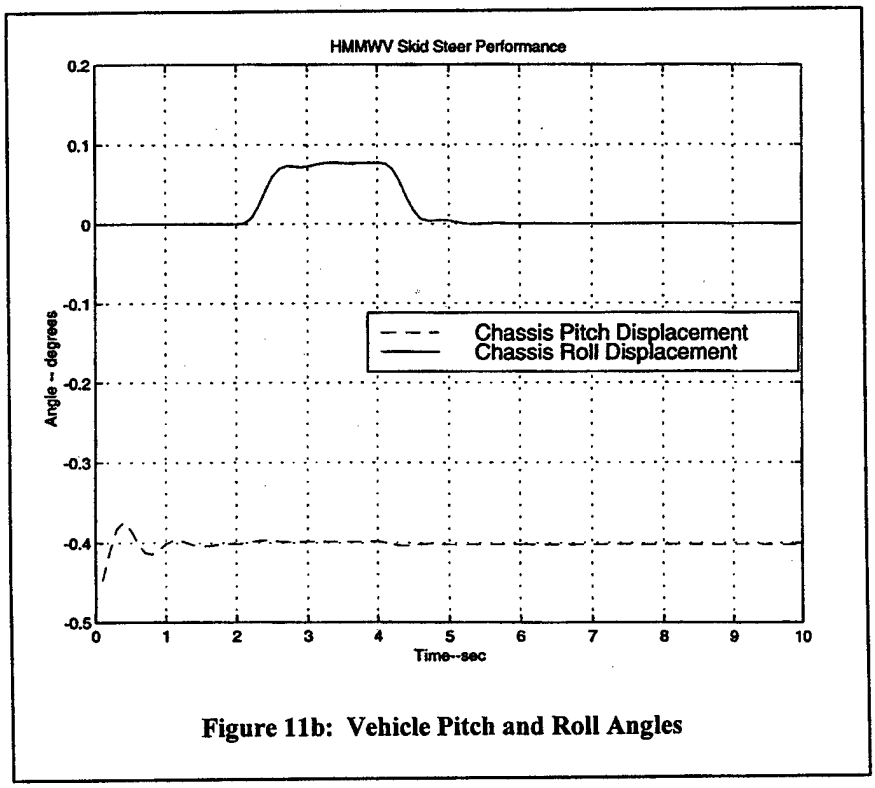


**Figure 11b: Vehicle Pitch and Roll Angles**

Figures 11a and 11b. Matlab simulation results with small turning torque for only 2 seconds and half the nominal tire cornering stiffness. a) front axle torque profiles (rear are identical); b) vehicle pitch and roll angle responses.

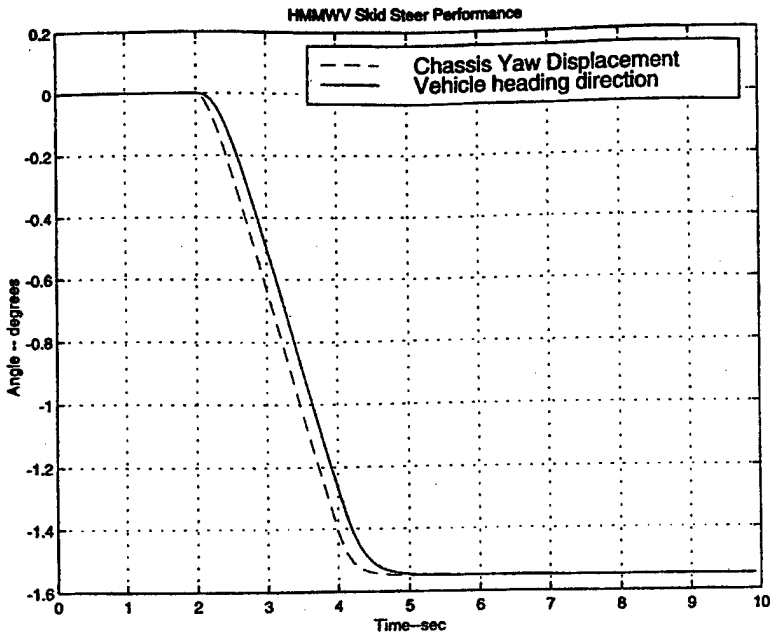


**Figure 11c: Vehicle Yaw and Heading Angles**

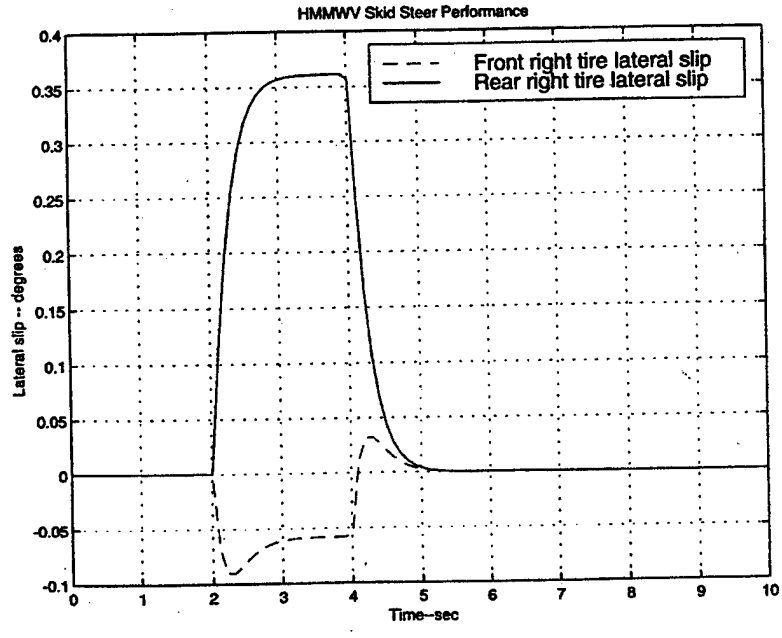


**Figure 11d: Front Axle Tire Side Slip Angles**

Figures 11c and 11d. Matlab simulation results with small turning torque for only 2 seconds and half the nominal tire cornering stiffness. c) vehicle yaw and heading angles; d) front axle tire side slip angles.